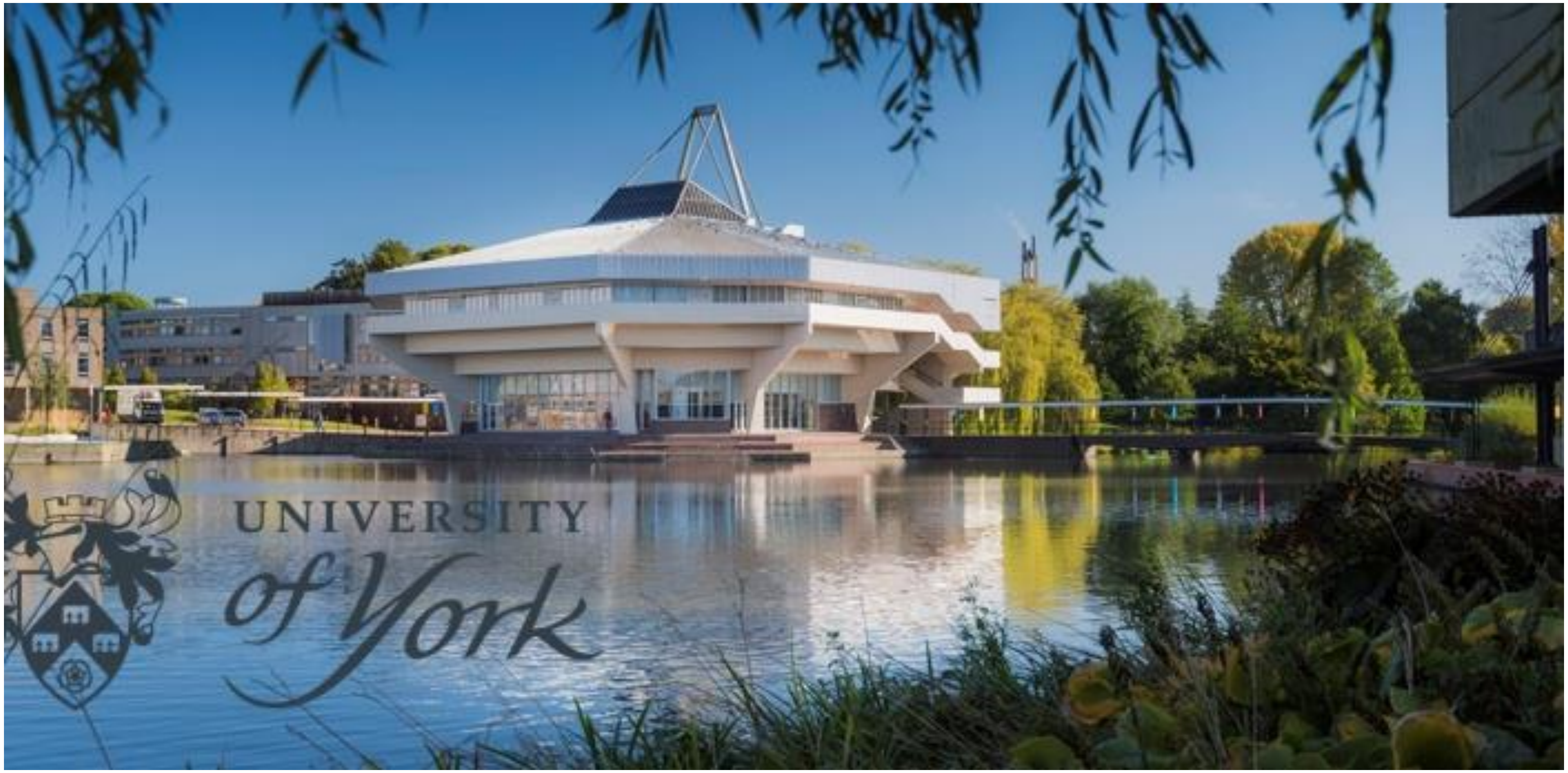

2024 European School on Magnetism

Magnetocaloric effect

Kelly Morrison

Loughborough University

Overview

1. **Context**
2. **Maxwell Relations**

   How can thermodynamics help us?
3. **Measurement Techniques**

   How can you measure the magnetocaloric effect?
4. **Materials**

   What benchmark values might we be comparing to?
5. **Universal Curves**

   What can universality tell us about a material system?
6. **Material Engineering**

   Beyond entropy change, what material properties should we be looking to improve?
7. **Future Outlook**

Rising Temperatures

Air conditioning and refrigeration accounts for 20% of electricity used in buildings today[1]

Refrigerants account for 7.8% total greenhouse gas emission

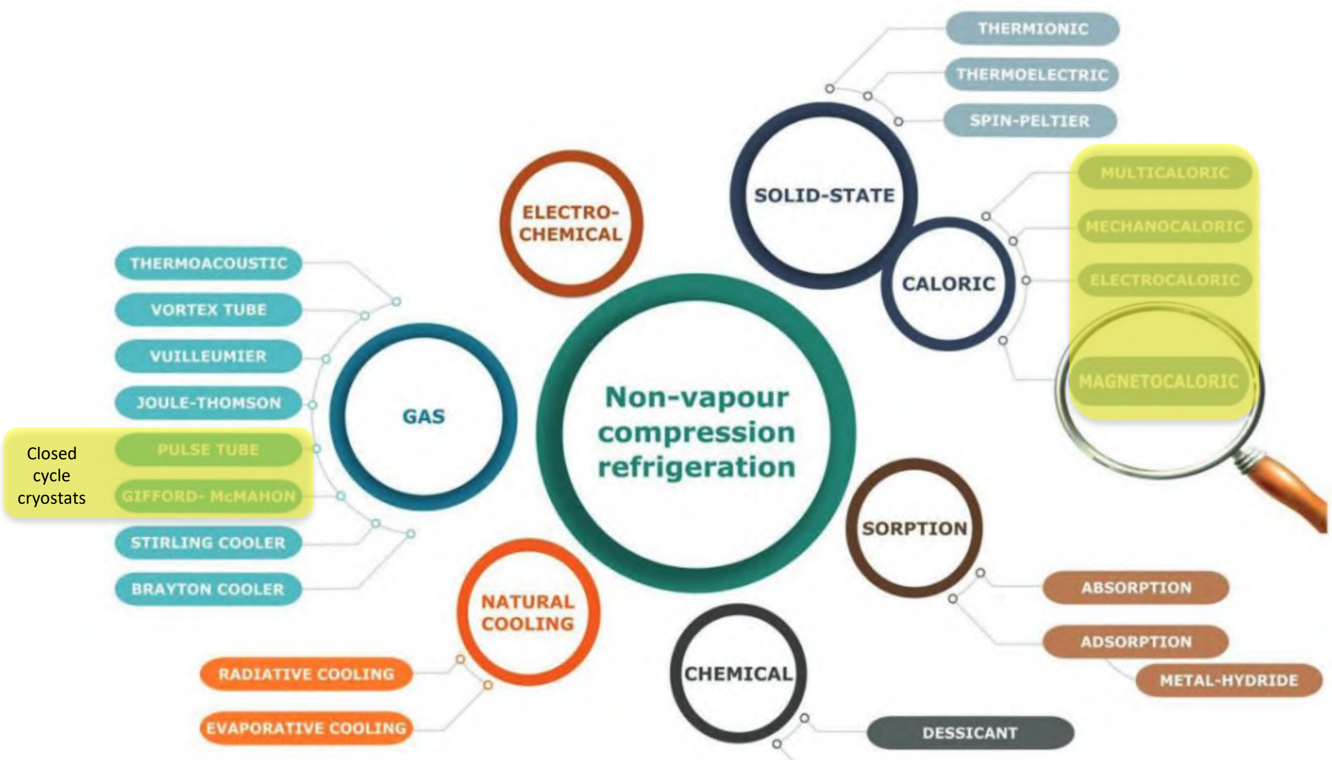

[2]

Figure 1. Non-vapor-compression refrigeration and air conditioning technologies.

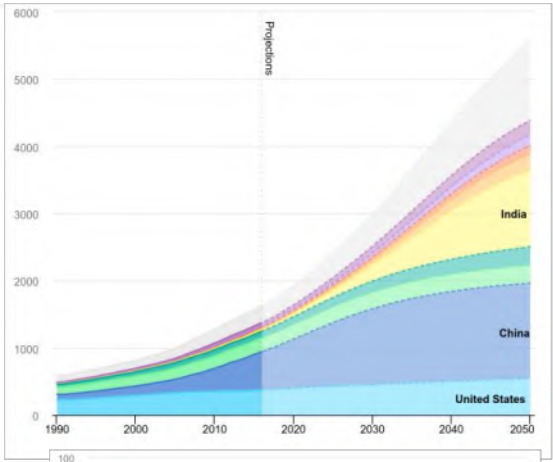

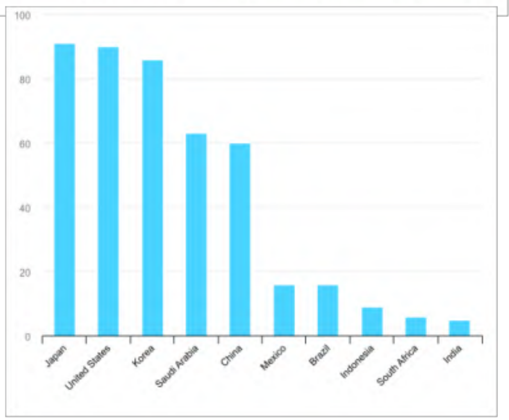

Want to know more?: See ESM 2021, Oliver Gutfleisch
Magneto (and multi-)caloric materials for efficient refrigeration

[1] International Energy Agency, The Future of Cooling, (2018), http://www.iea.org/reports/the-future-of-cooling
[2] A. Kitanovski, *Adv. Energy Materials* **10** 1903741 (2020)

Magnetic Cooling

[CONTRIBUTION FROM THE CHEMICAL LABORATORY OF THE UNIVERSITY OF CALIFORNIA]

A THERMODYNAMIC TREATMENT OF CERTAIN MAGNETIC EFFECTS. A PROPOSED METHOD OF PRODUCING TEMPERATURES CONSIDERABLY BELOW 1° ABSOLUTE

BY W. F. GIAUQUE

RECEIVED DECEMBER 14, 1926 PUBLISHED AUGUST 5, 1927

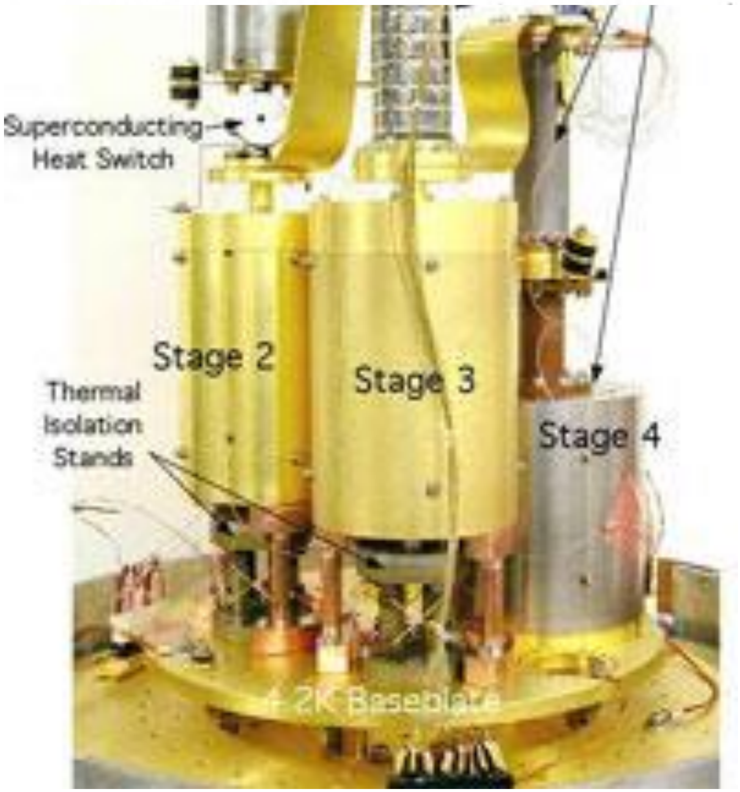

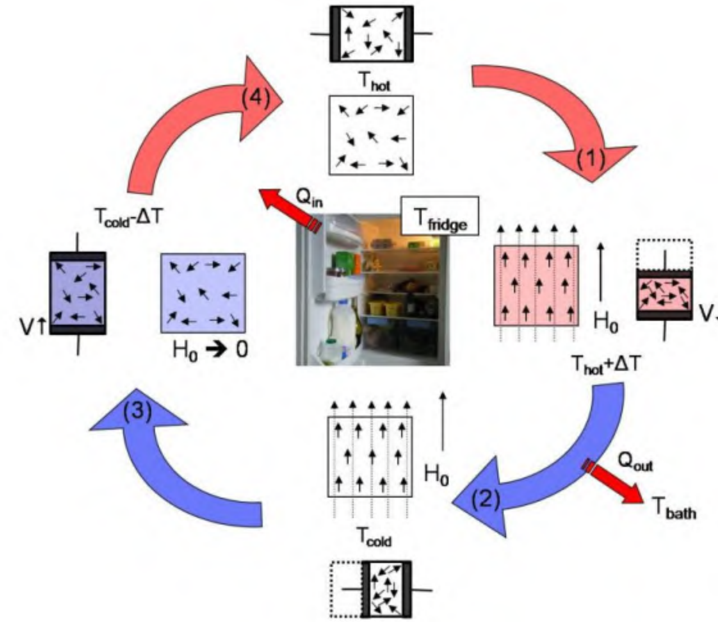

"Photograph of technology demonstration of a Continuous Adiabatic Demagnetization Refrigerator developed at NASA's Goddard Space Flight Center."
[Figure taken from http://ixo.gsfc.nasa.gov/technology/xms.html]

Anders Smith – Who discovered the magnetocaloric effect?, Eur. Phys. J. H 38 507-517 (2013)

Magnetic Cooling

VOLUME 78, NUMBER 23 PHYSICAL REVIEW LETTERS 9 JUNE 1997

Giant Magnetocaloric Effect in $Gd_5(Si_2Ge_2)$

V. K. Pecharsky and K. A. Gschneidner, Jr.
Ames Laboratory and Department of Materials Science and Engineering, Iowa State University, Ames, Iowa 50011-3020
(Received 22 November 1996)

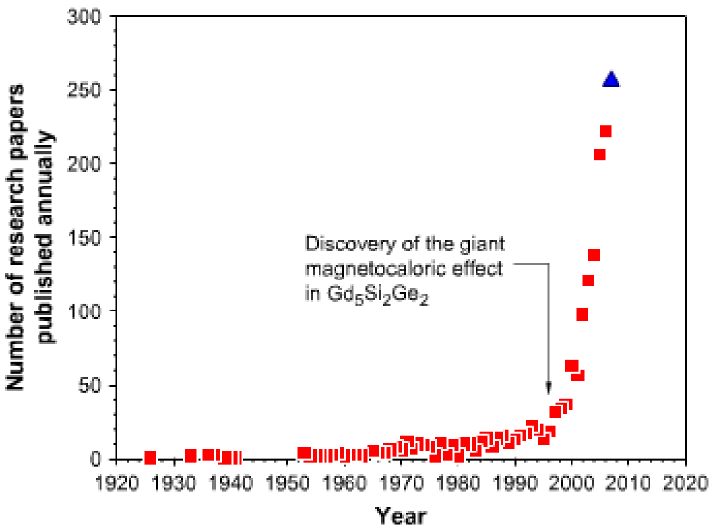

Fig. 1 – The number of research papers published annually over the past 80 years containing the word "magnetocaloric" in the title, abstract, or among the keywords. The values for 2007 (triangle) are based on the number of papers abstracted during the first three-fourths of the year.

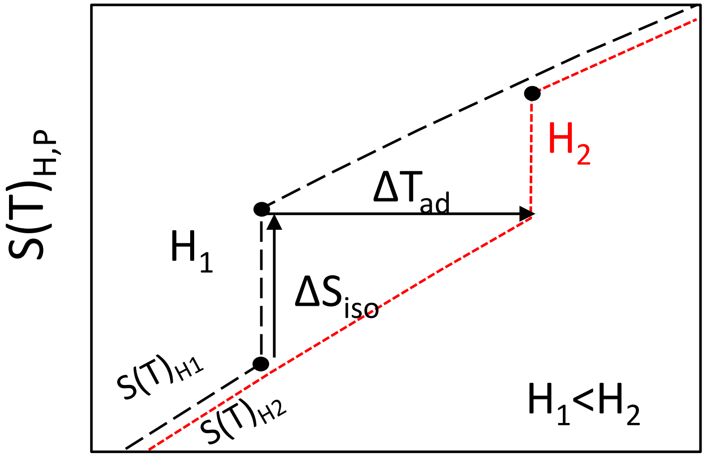

$$\Delta T_{ad}(T,\Delta H) \approx -\frac{T\Delta S(T)}{C(T)}$$

Refrigerant capacity ~ $\Delta S.\Delta T_{ad}$

Research Aims

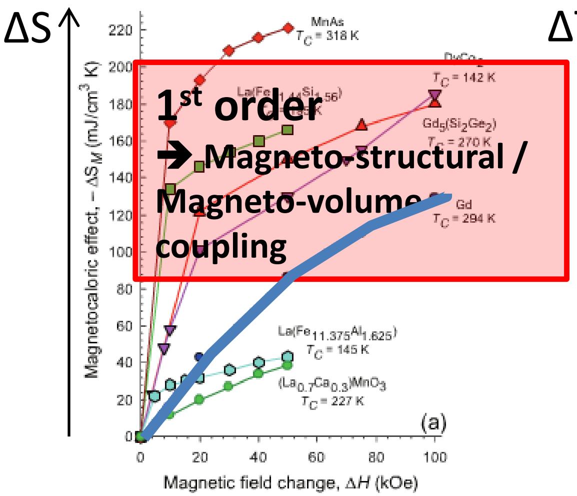

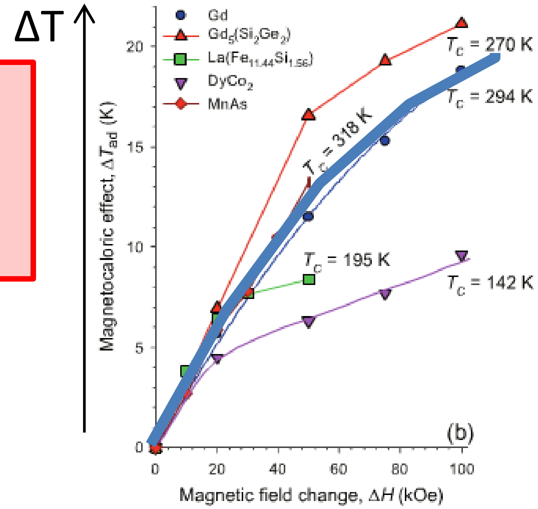

- ΔS , ΔT_{ad}
- H_c, ΔH
- Cost
- Manufacturability
- Tunability

2011 – Camfridge prototype attained T_{span} ~ 35K with $La(Fe,Si,Co)_{13}$ plates.

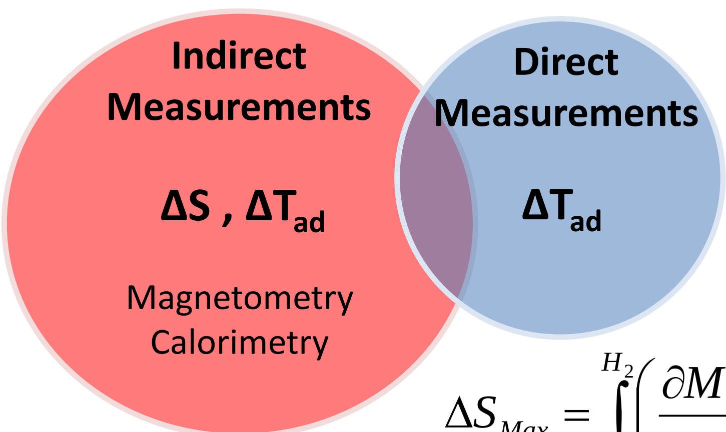

$$\Delta S_{Max} = \int_{H_1}^{H_2} \left(\frac{\partial M(T,H)}{\partial T} \right)_H dH$$

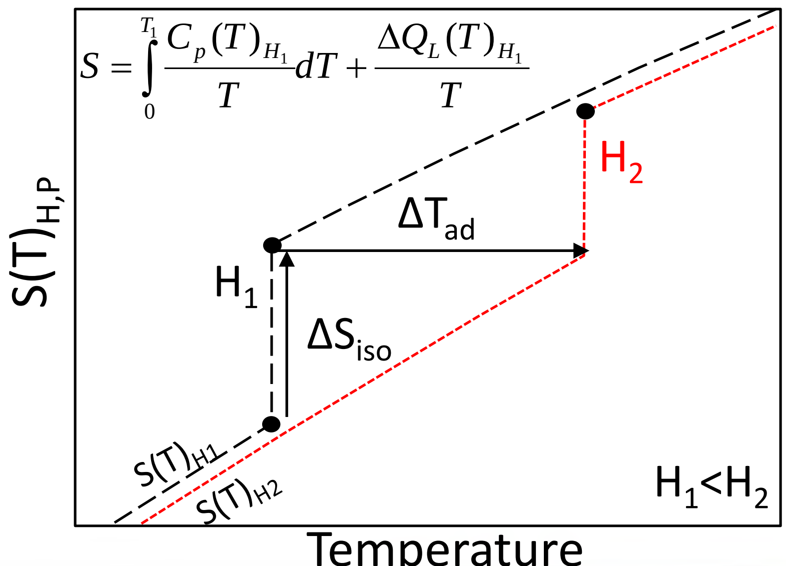

V.K. Pecharsky *et. al.*, *Phys Rev. B* **64** 144406 (2001)
K.A. Gschneidner et al, Rep. Prog. Phys. **68**, 1479-1539 (2005)

Maxwell Relations

$$dG = -SdT - MdH + VdP$$

$$\left(\frac{\partial S}{\partial H}\right)_{T,P} = \left(\frac{\partial M}{\partial T}\right)_{H,P}$$

$$\left(\frac{\partial S}{\partial P}\right)_{T,H} = -\left(\frac{\partial V}{\partial T}\right)_{H,P}$$

$$\left(\frac{\partial M}{\partial P}\right)_{H,T} = -\left(\frac{\partial V}{\partial H}\right)_{T,P}$$

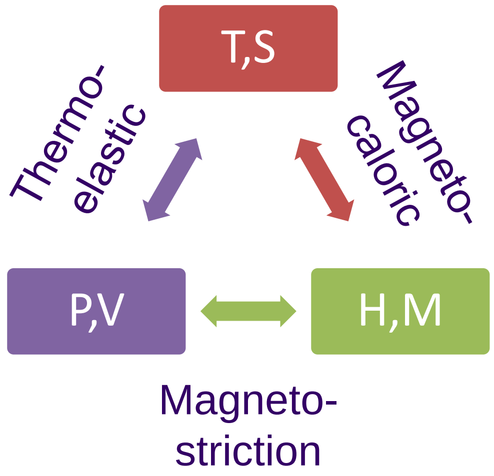

Equation of state:

$$\frac{H}{M} = A + BM^2 + CM^4$$

Maxwell Relations

$$dU = TdS + HdM - PdV$$

$$dG = -SdT - MdH + VdP$$

$$\left(\frac{\partial G}{\partial T}\right)_{H,P} = -S \quad \Rightarrow \quad \frac{\partial}{\partial H}\left(\frac{\partial G}{\partial T}\right)_{H,P} = -\left(\frac{\partial S}{\partial H}\right)_{T,P}$$

$$\left(\frac{\partial G}{\partial H}\right)_{T,P} = -M \quad \Rightarrow \quad \frac{\partial}{\partial T}\left(\frac{\partial G}{\partial H}\right)_{T,P} = -\left(\frac{\partial M}{\partial T}\right)_{H,P}$$

$$\left(\frac{\partial G}{\partial P}\right)_{T,H} = V$$

$$\frac{\partial}{\partial H}\left(\frac{\partial G}{\partial T}\right) = \frac{\partial}{\partial T}\left(\frac{\partial G}{\partial H}\right)$$

$$\therefore \quad -\left(\frac{\partial S}{\partial H}\right)_{T,P} = -\left(\frac{\partial M}{\partial T}\right)_{H,P}$$

$$\Delta S_{Max} = \int_{H_1}^{H_2} \left(\frac{\partial M(T,H)}{\partial T}\right)_H dH$$

Similarly

$$-\left(\frac{\partial S}{\partial P}\right)_{H,T} = \left(\frac{\partial V}{\partial T}\right)_{H,P}$$

$$-\left(\frac{\partial M}{\partial P}\right)_{H,P} = \left(\frac{\partial V}{\partial H}\right)_{T,P}$$

Magnetometry: Potential problems

Magnetometry - See ESM 2024, Stuart Cavill.
Magnetic measurement instruments and techniques

Same sample measured 2 different ways.
Why so different?

$$\Delta S_{Max} = \int_{H_1}^{H_2} \left(\frac{\partial M(T,H)}{\partial T} \right)_H dH$$

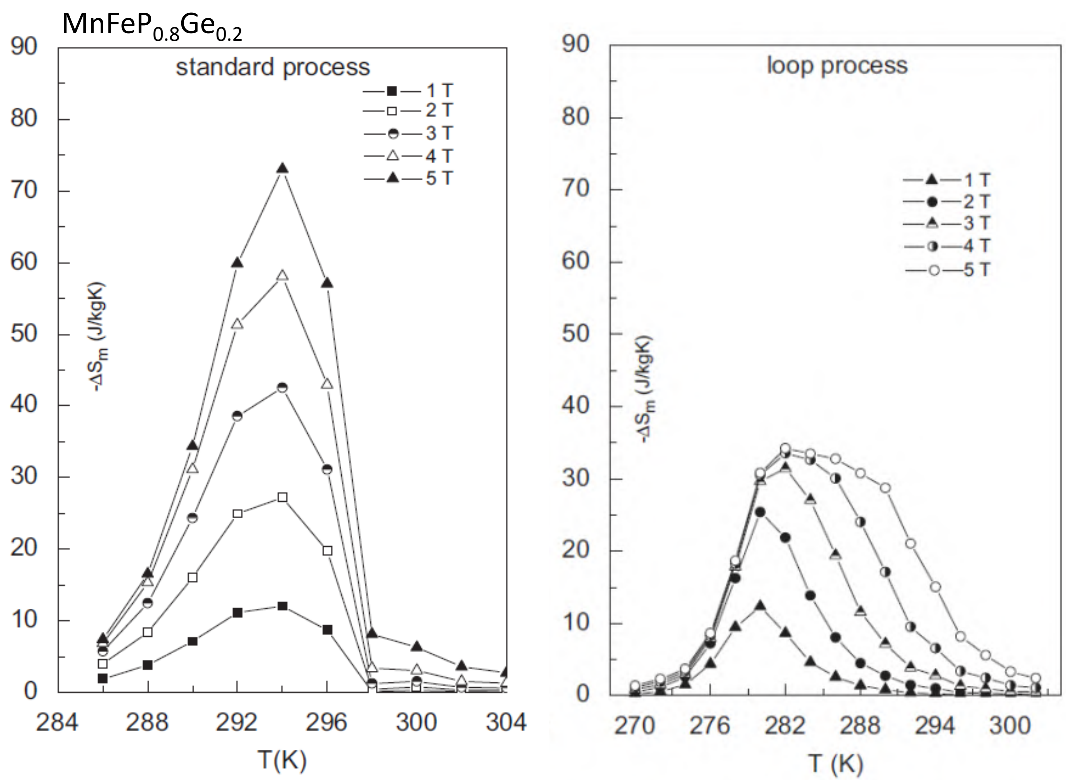

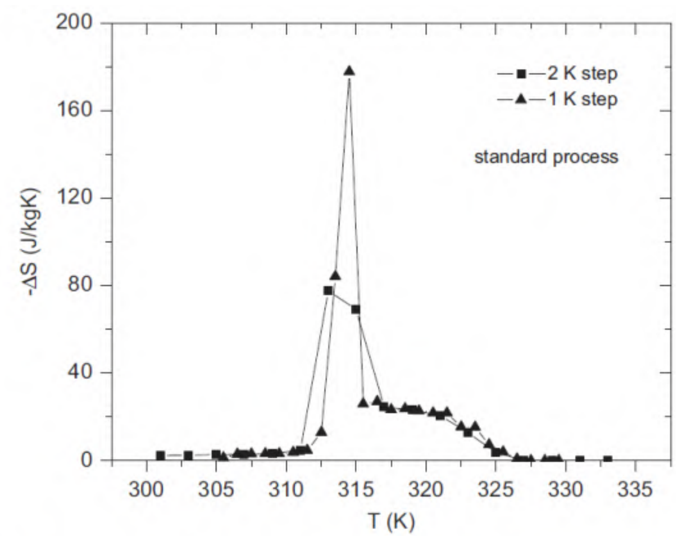

Fig. 9. (a) Magnetization isotherms measured according to the standard process. (b) Entropy change as a function of temperature for $Mn_{0.99}Cu_{0.01}As$ for 1 and 2 K steps for a 5 T field change.

L. Caron et al., J. Magn. And Magn. Mater. **321**, 3559-3566 (2009)

Magnetometry: Field History

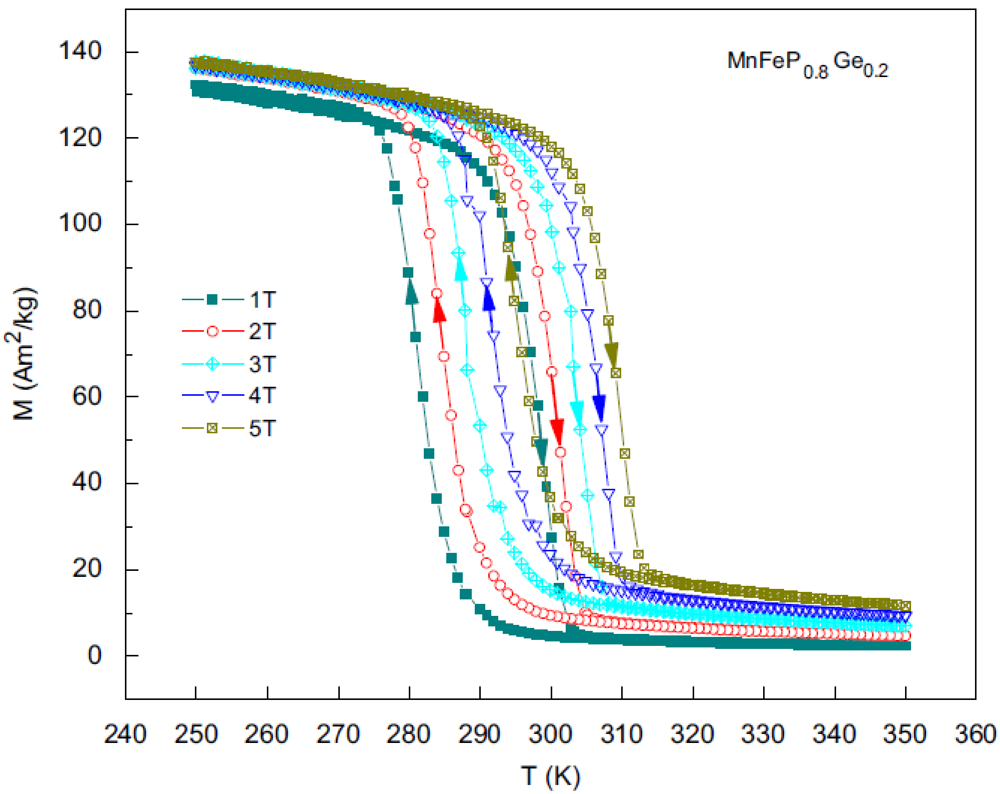

Fig. 1. Temperature dependence of the magnetization of $MnFeP_{0.8}Ge_{0.2}$ measured in constant fields of 1, 2, 3, 4 and 5 T with temperature increasing and decreasing in a step of 2 K, the arrows indicate the warming and cooling processes.

$$\Delta S_{Max} = \int_{H_1}^{H_2} \left(\frac{\partial M(T,H)}{\partial T} \right)_H dH$$

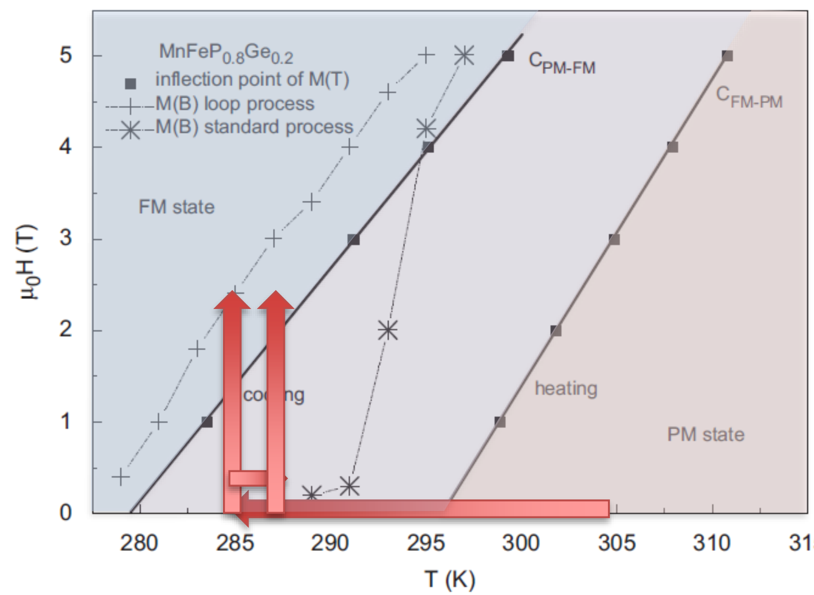

Fig. 2. Magnetic phase diagram of the compound $MnFeP_{0.8}Ge_{0.2}$ as derived from isofield magnetization measurements shown in Fig. 1 ■ (other symbols derived from M(B) see Figs. 3(a) and 4(a)).

Magnetometry

Constructing isofield M(T) from isothermal M(H) data requires consideration of field history where there is thermal/field hysteresis.

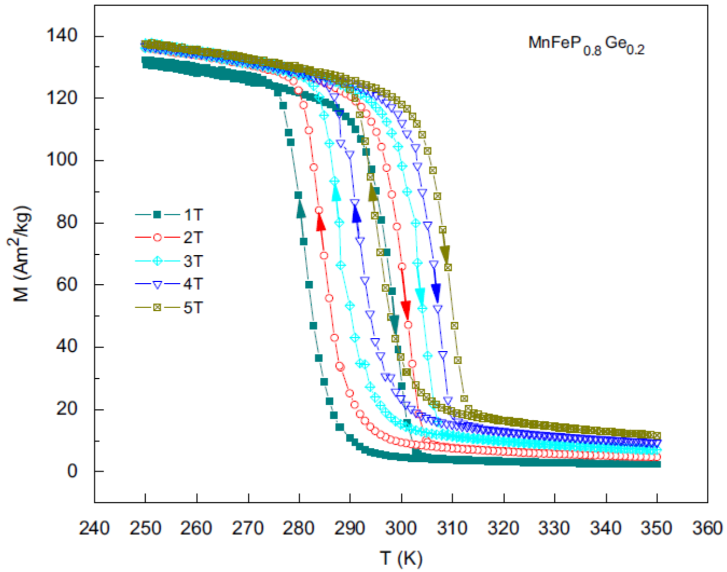

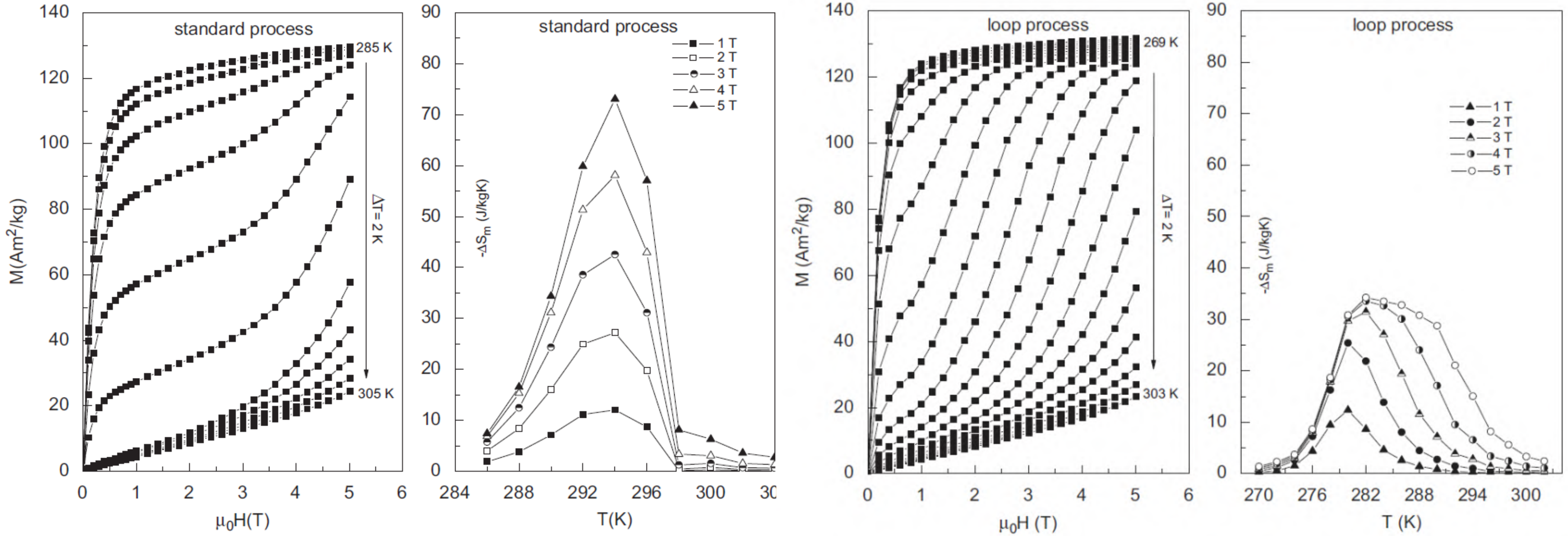

L. Caron et al., J. Magn. And Magn. Mater. **321**, 3559-3566 (2009)

Magnetometry: Round Robin

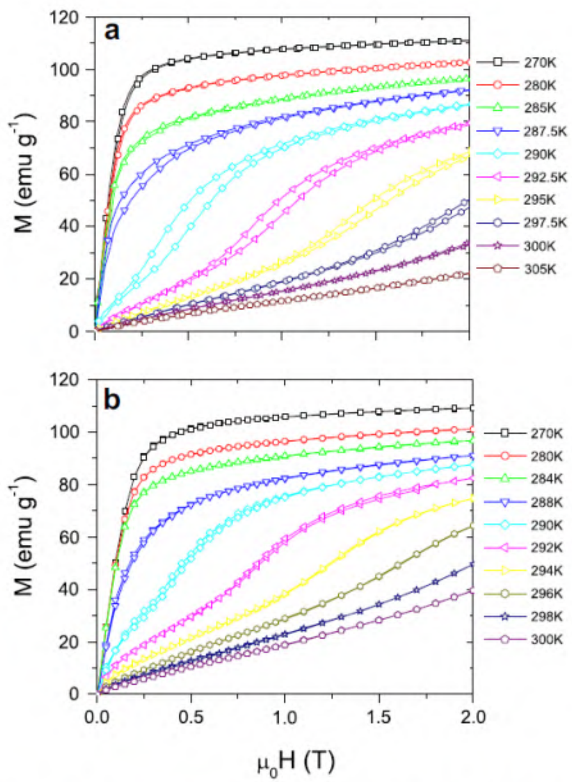

Fig. 3 – Magnetisation versus applied field for the MCP1011 sample (colour online). Data taken at (a) Imperial College (IC) using an Oxford Instruments vibrating sample magnetometer, (saturation magnetisation 112 emu.g^{-1} at 270 K and 2 T) and (b) IFW using a PPMS SQUID magnetometer (saturation magnetisation 110 emu.g^{-1} at 270 K and 2 T).

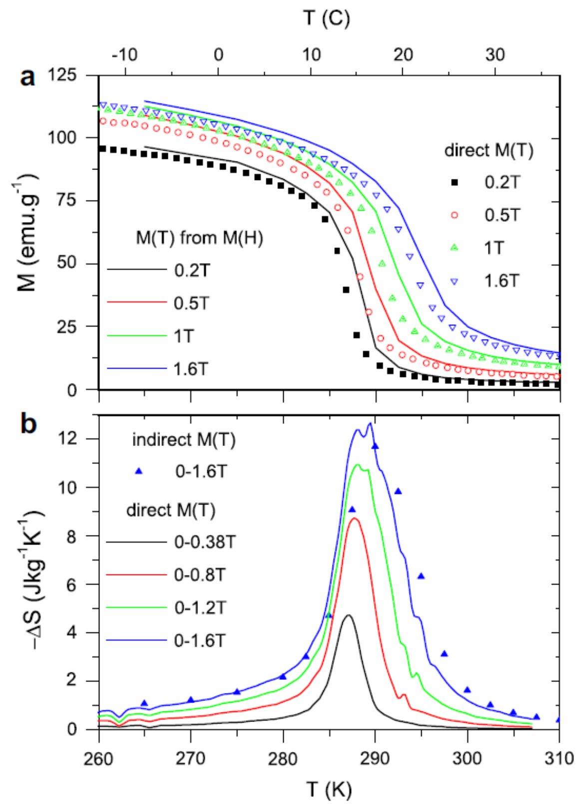

Fig. 4 – Entropy change determined from magnetisation measurements (colour online). (a) $M(T)$ curves measured directly (VAC) and extracted from $M(H)$ curves (IC/IFW). (b) The entropy change ΔS calculated from the $M(T)$ curves shown in (a).

Calorimetry: Potential Problems

Phase diagram:	Effect of temperature/pressure
Thermal history:	"Isothermal" measurements
Timescales:	Driving frequency
	Thermal conductivity
	Equipment limitations
Data analysis:	Limitations of model used

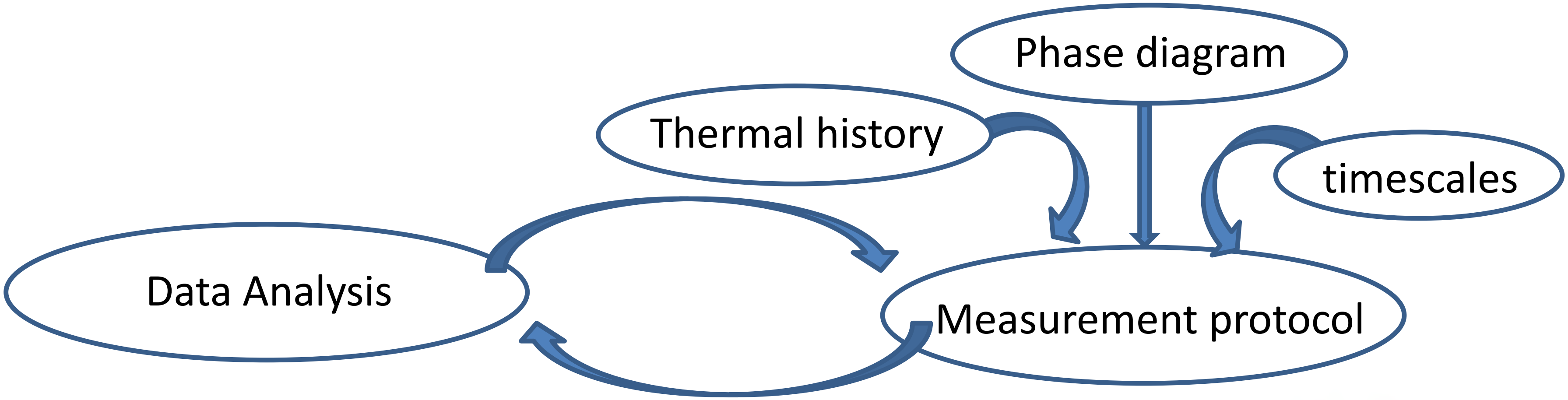

Differential Scanning Calorimetry (DSC)

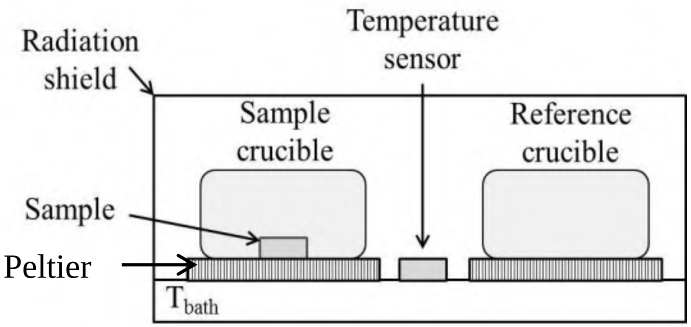

Heat flow measured.
Temperature scanned.

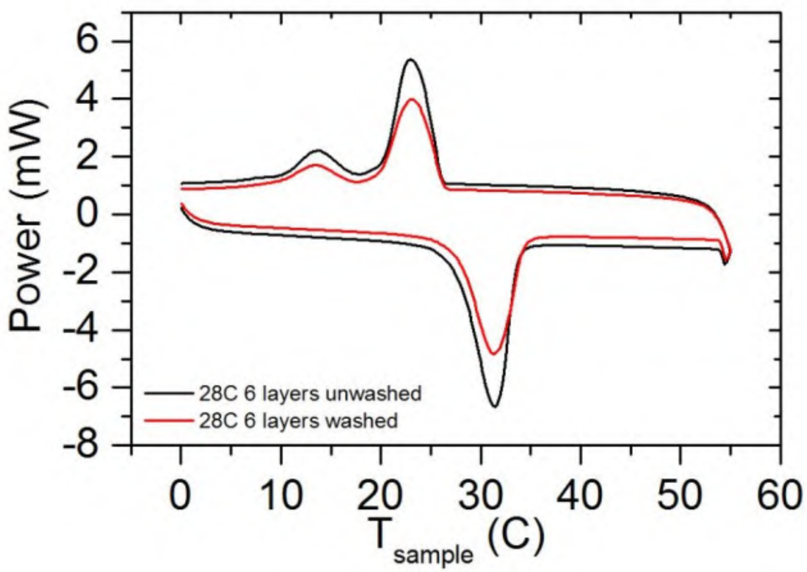

Power supplied to sample
(to keep it at same temperature as reference)

Heat capacity

$$C_p = \frac{P}{\dot{T} m}$$

Heating rate

mass

Relaxation Calorimetry

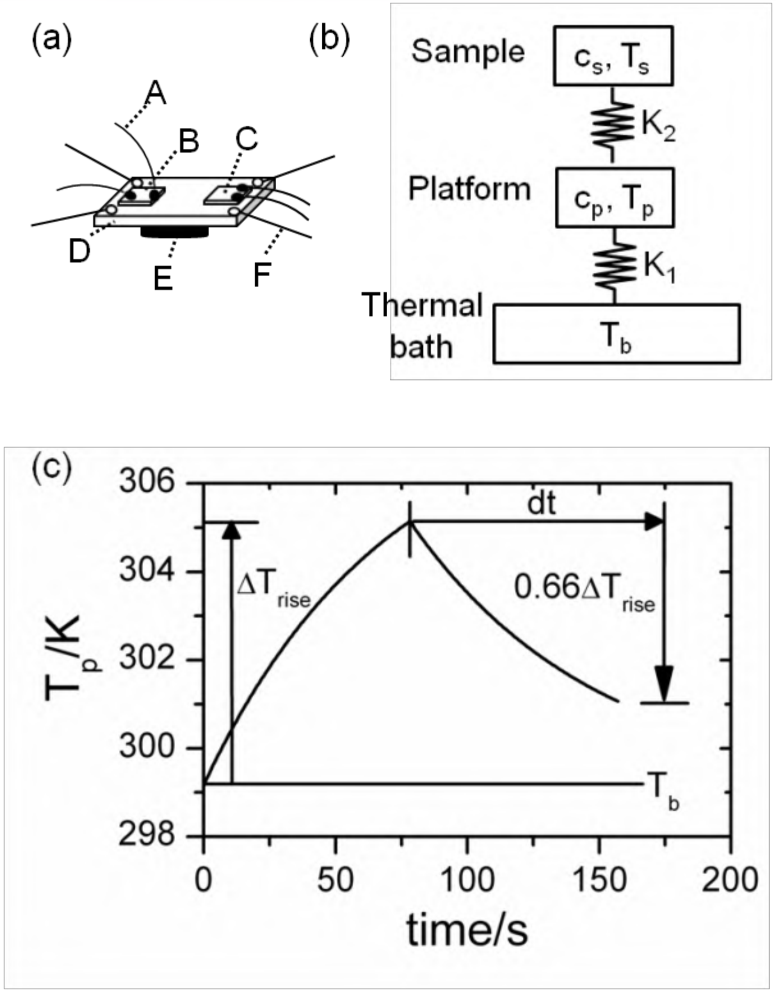

e.g. Quantum Design PPMS with heat capacity option

The PPMS heat capacity option: Curve fitting method[1]

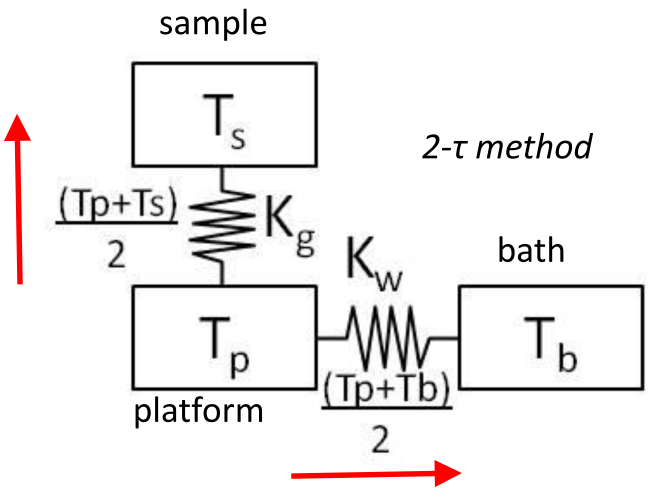

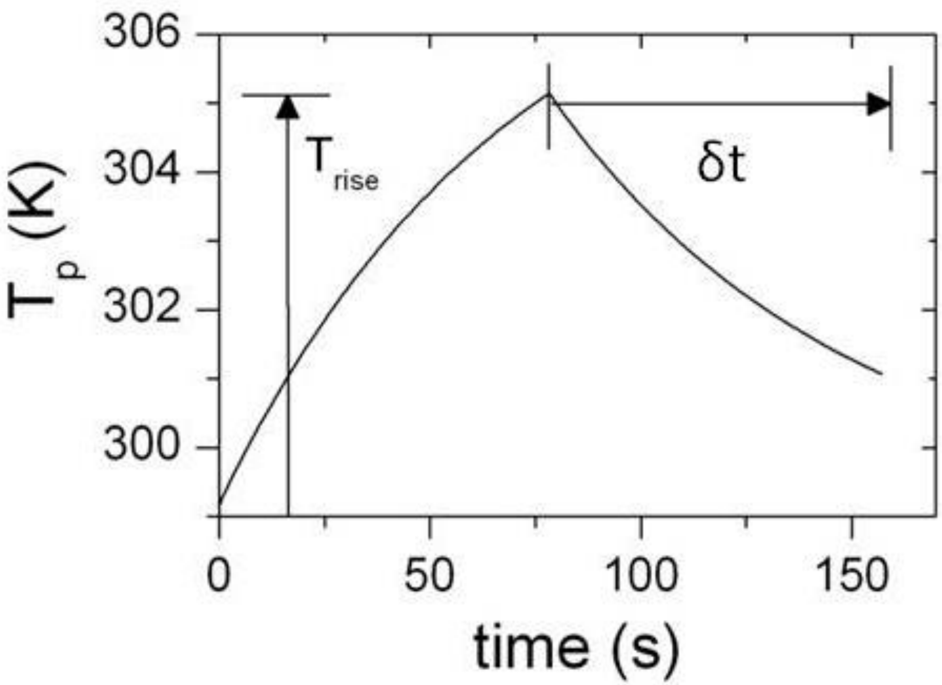

One relaxation curve gives you:

1. 1 data point averaged over T_{rise}
2. K_w
3. K_g

Sharp changes in heat capacity, or latent heat can result in poor measurement

The PPMS heat capacity option: Curve fitting method[1]

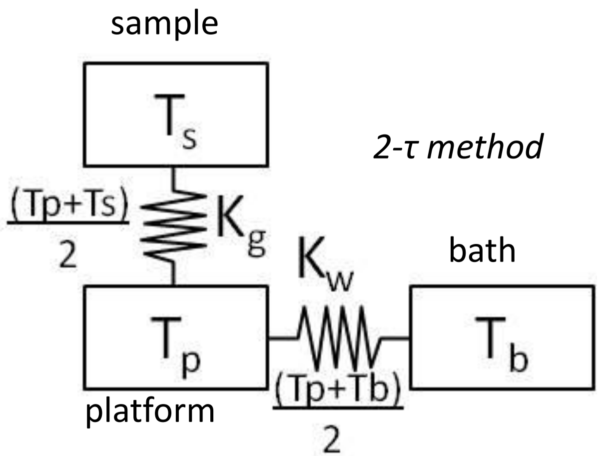

Example[1]

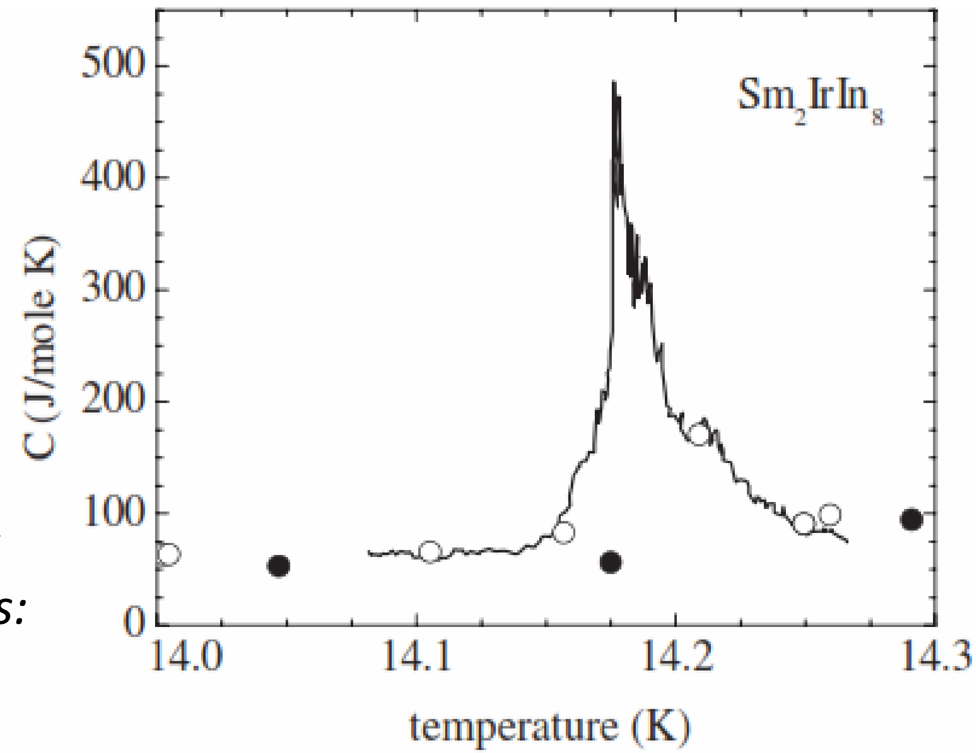

Evaluate same relaxation curve at every point using K_w,K_g and following equations:

$$C_s = \left[-C_p \frac{dT_p}{dt} + K_w[T_p(t) - T_b] + P(t) \right] \times \frac{dt}{dT_s}$$

$$T_s = \frac{C_p \frac{dT_p}{dt} + K_w[T_p - T_b] - P(t)}{K_g} + T_p(t)$$

[1]J.C. Lashley *et al.,* Cryogenics **43** 369-378 (2003)
H. Suzuki *et al.*, Cryogenics **50** 693–699 (2010)

Measurement techniques: round robin study

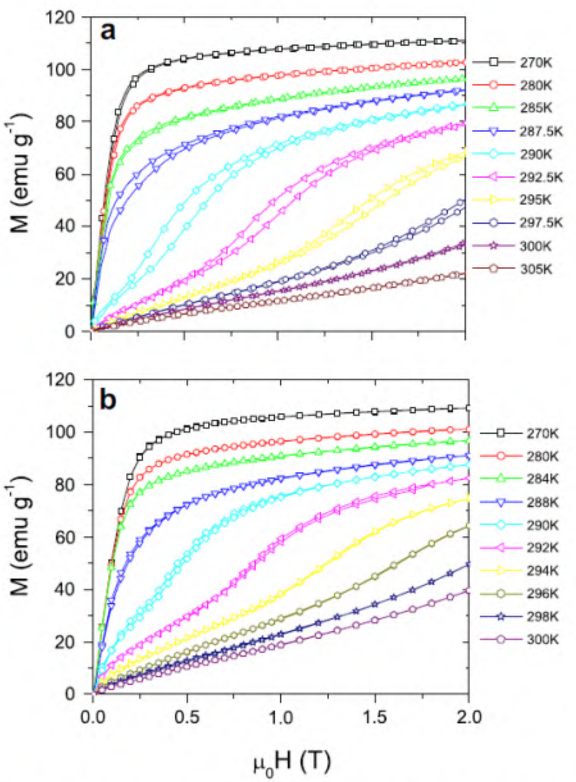

Fig. 3 – Magnetisation versus applied field for the MCP1011 sample (colour online). Data taken at (a) Imperial College (IC) using an Oxford Instruments vibrating sample magnetometer, (saturation magnetisation 112 emu.g^{-1} at 270 K and 2 T) and (b) IFW using a PPMS SQUID magnetometer (saturation magnetisation 110 emu.g^{-1} at 270 K and 2 T).

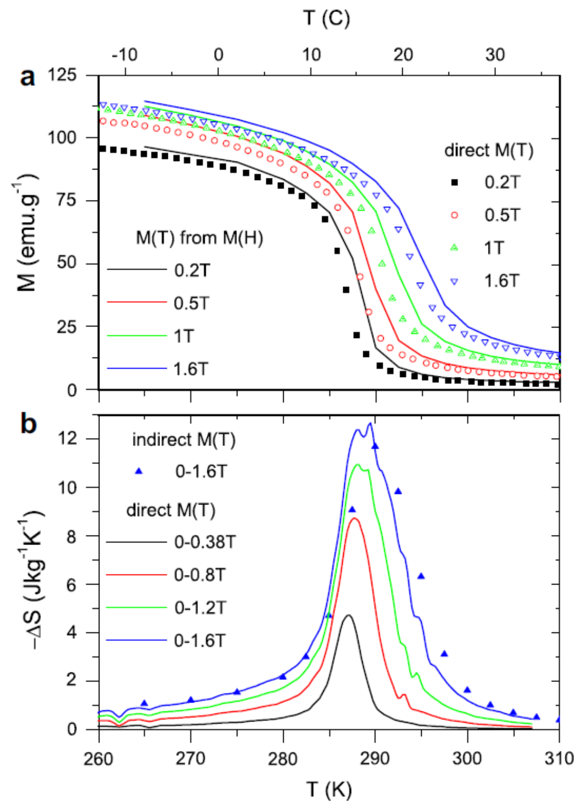

Fig. 4 – Entropy change determined from magnetisation measurements (colour online). (a) *M(T)* curves measured directly (VAC) and extracted from *M(H)* curves (IC/IFW). (b) The entropy change ΔS calculated from the *M(T)* curves shown in (a).

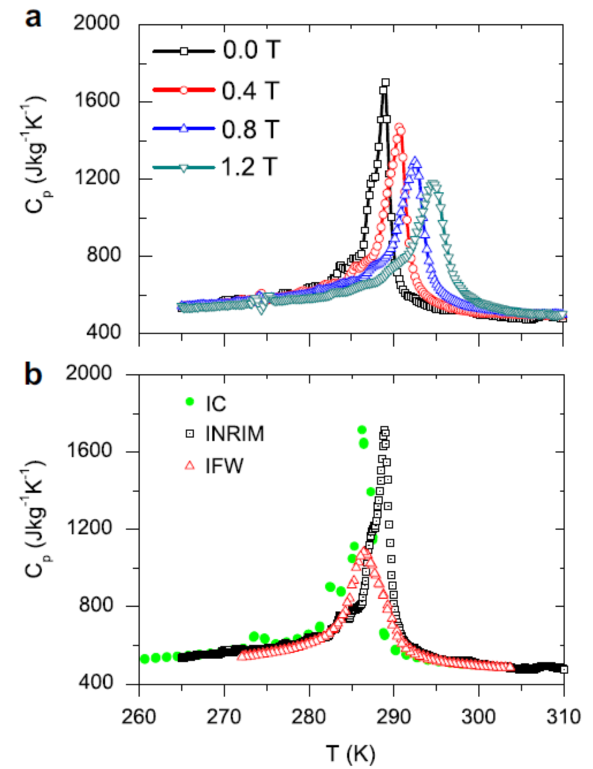

Fig. 5 – Heat capacity data for the MCP1011 sample (colour online). (a) INRIM data taken in various fixed external fields, and (b) heat capacity in zero field: a comparison of heat capacity measured in three laboratory environments using different methods.

Want to know more?: See ESM 2019, Vittorio Basso.
Indirect techniques: calorimetry, dilatometry, transport

K. Morrison *et al.*, *Int. J. Refrig.* **35**, 1528 (2012)

Giant Magnetocaloric Effect in $Gd_5(Ge_xSi_{1-x})_4$

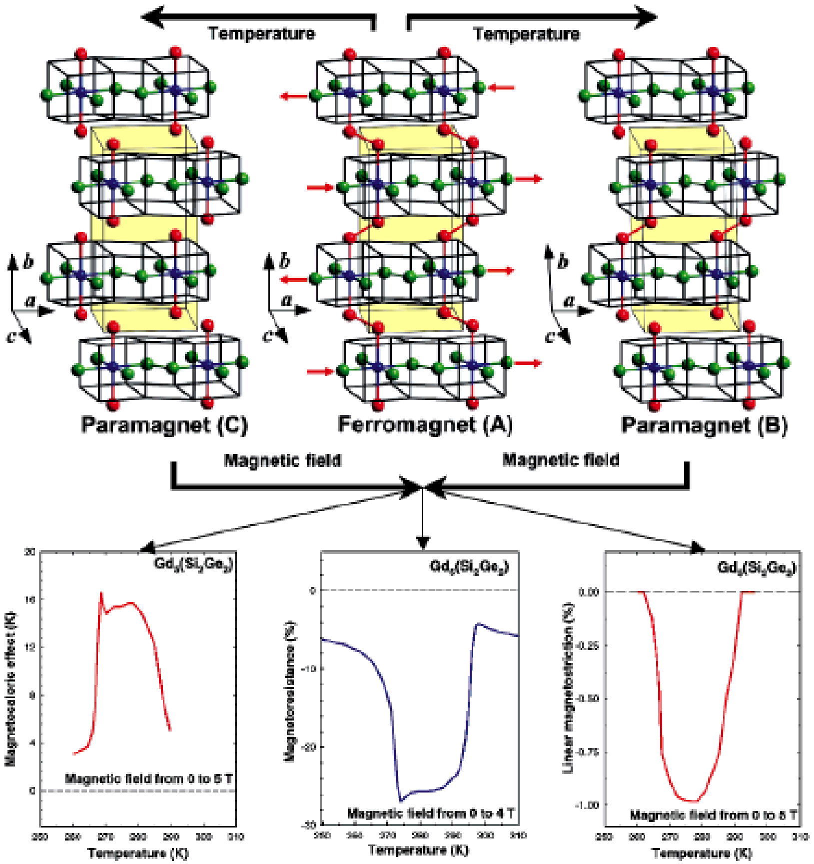

Fig. 3. Correlation between the magnetic responses of the $Gd_5(Si_xGe_{1-x})_4$ materials and their crystal structures for $0 \le x \le 0.5$. At low temperatures the compounds are ferromagnetic (A) with all slabs (light blue) connected via the Si(Ge)–Si(Ge) covalent bonds. Depending on the composition, the materials become paramagnetic with either one-half (B) or none (C) of the slabs connected above the Curie temperatures as shown by long horizontal arrows at the top of the figure. The transitions from state A to B or A to C are coupled with shear movement of the slabs by −0.8 (A → B) or −1.1 Å (A → C) as indicated by red horizontal arrows. When a magnetic field is applied above Curie temperature, the reverse magnetic–martensitic transitions occur (B → A or C → A, as shown by long horizontal arrows in the middle) resulting in the giant magnetocaloric effect, giant magnetoresistance, and colossal magnetostriction. These are shown at the bottom of the figure for the $Gd_5(Si_2Ge_2)$ composition (i.e., for $x = 0.5$). The unit cells of the three crystallographic modifications existing in the $Gd_5(Si_xGe_{1-x})_4$ system are highlighted in yellow.

ADVANCED MATERIALS

$Gd_5(Si_xGe_{1-x})_4$: An Extremum Material**

By *Vitalij K. Pecharsky** and *Karl A. Gschneidner Jr.*

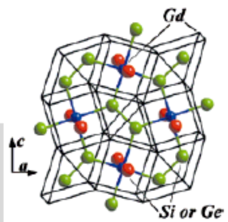

The large shear displacements of atomic layers in $Gd_5(Si_xGe_{1-x})_4$ materials, coupled with the change of crystallographic symmetry and magnetic order, characterizes these transformations as magnetic–martensitic, which are extremely rare. The start and the end of the magnetic–martensitic transitions depends strongly on the direction of change (i.e., increasing or decreasing) of either or both the temperature and magnetic field. These profound bonding, structural, electronic, and magnetic changes, which occur in the $Gd_5(Si_xGe_{1-x})_4$ system, bring about some extreme changes of the materials' behavior resulting in a rich variety of unusually powerful magneto-responsive properties, such as the giant magnetocaloric effect, colossal magnetostriction, and giant magnetoresistance.

Adv. Mater. **2001**, *13*, No. 9, May 3

Paramagnetic - Monoclinic
Ferromagnetic - Orthorhombic

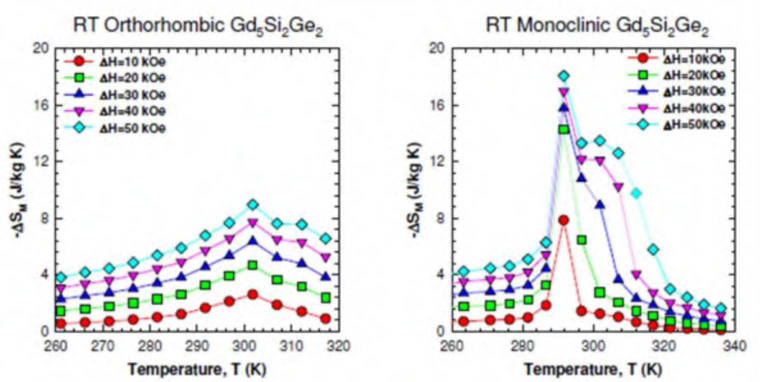

Same alloy, different heat treatments to obtain the two structures.

Courtesy of K.A. Gschneidner

Magneto-structural Coupling

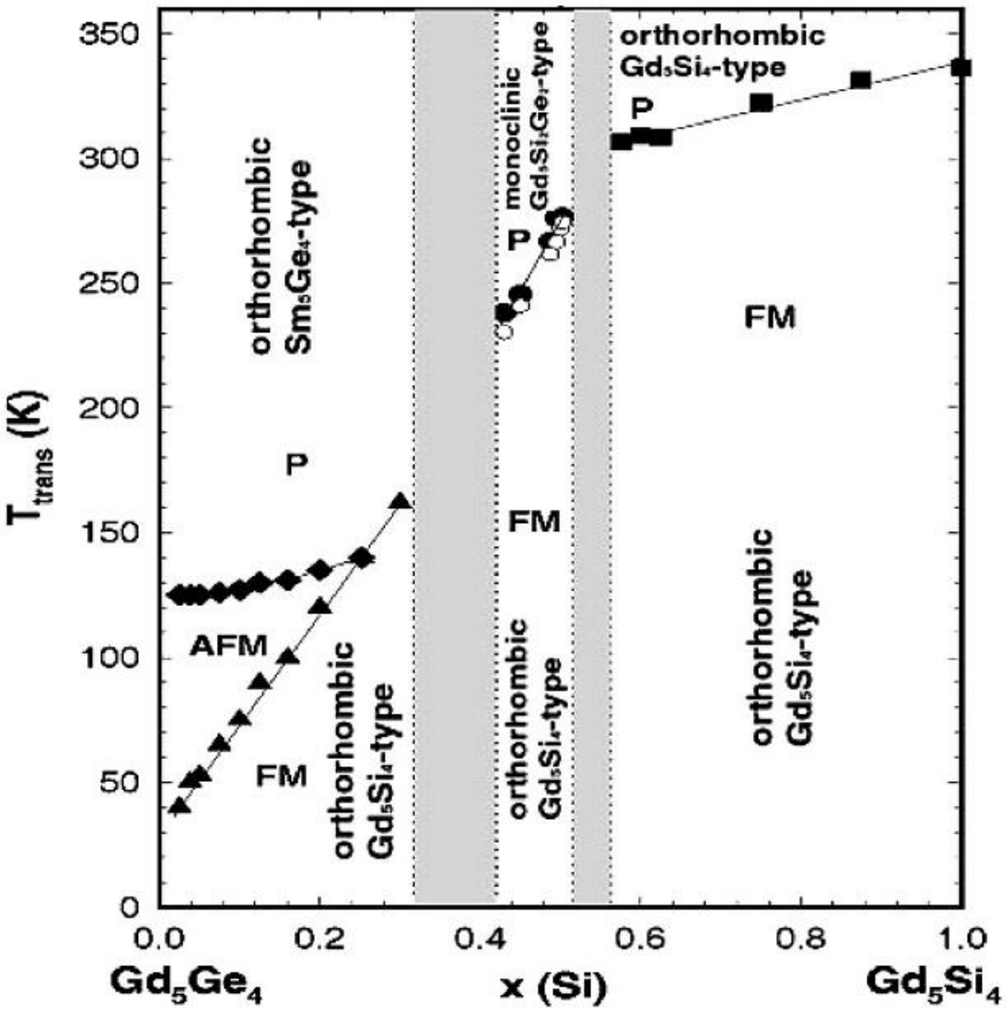

Gd_5Ge_4

>20 K AFM-FM

<20K Magnetic glass

T_N~130 K

$Gd_5Si_2Ge_2$

T_C ~275 K:

FM-PM +

orthorhombic-monoclinic

A.O. Pecharsky *et al. J. Alloys. Comp.* 338, 126-135 (2002)

$Gd_5Ge_2Si_2$ Single Crystal

a axis

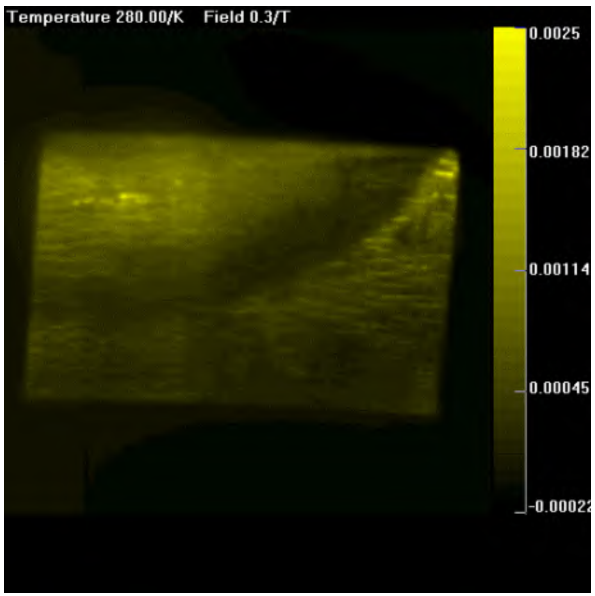

b axis

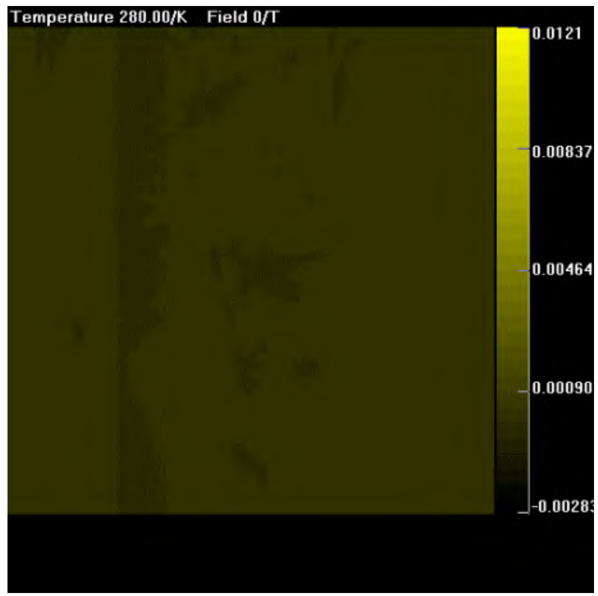

c axis

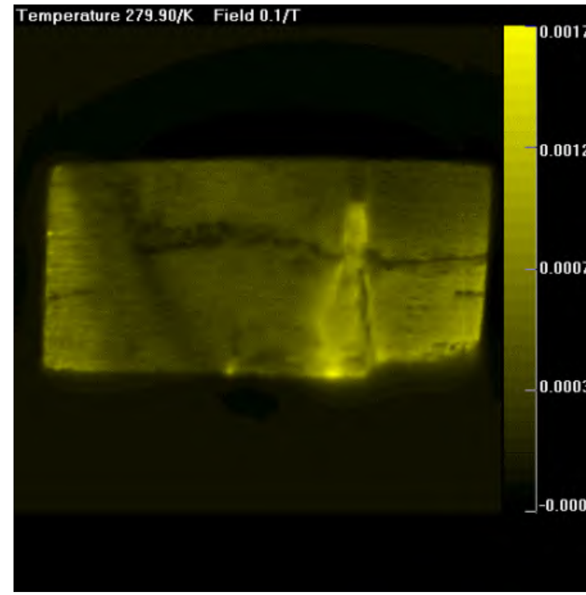

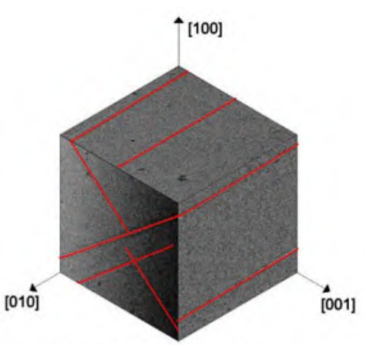

Digitally rendered 3-D image of a single crystal $Gd_5Si_2Ge_2$

Imperial College London

$Gd_5Ge_2Si_2$ Single crystal

- Platelets of $Gd_5(Ge_xSi_{1-x})_3$
- Criss-cross pattern in [010] b-face
- Stripe pattern in [100] a- and [001] c-face

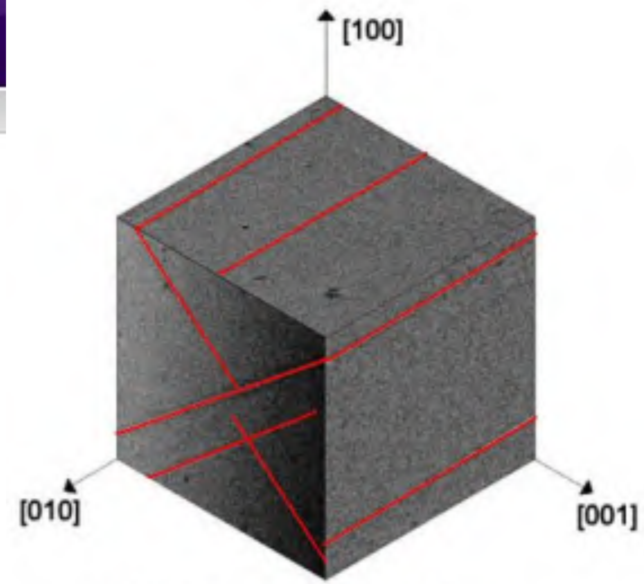

Digitally rendered 3-D image of a single crystal $Gd_5Si_2Ge_2$

How does presence of platelets affect AFM-FM transition?

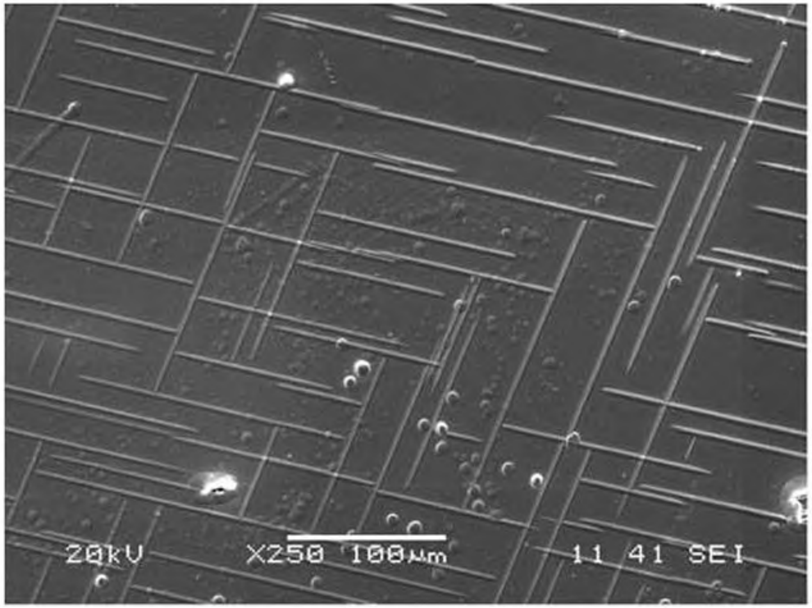

SEM micrograph of an ion-etched oriented $Gd_5Si_2Ge_2$ single crystal

O. Ugurlu, et al., Acta Mater. 53, 3525-3533 (2005)

$Gd_5Ge_2Si_2$ Single Crystal

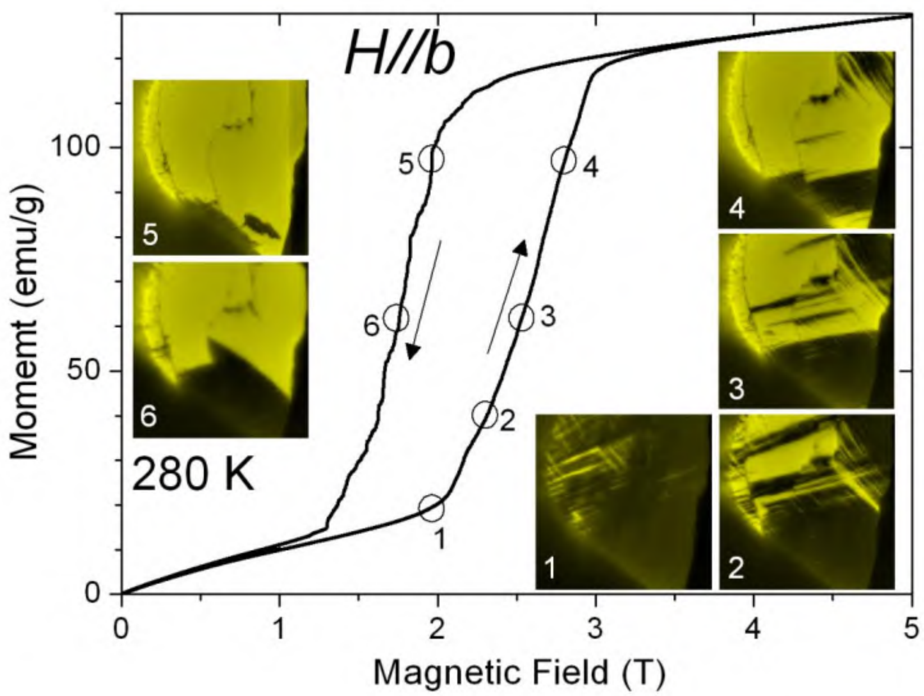

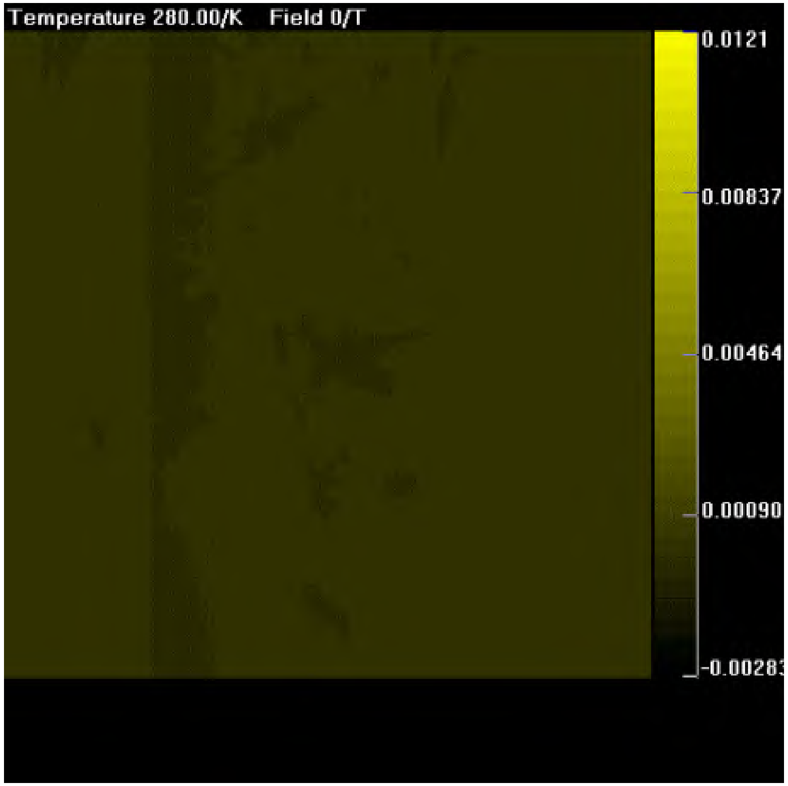

Presence of PM platelets seed the phase transition.

$Gd_5Ge_2Si_2$ Microcalorimetry

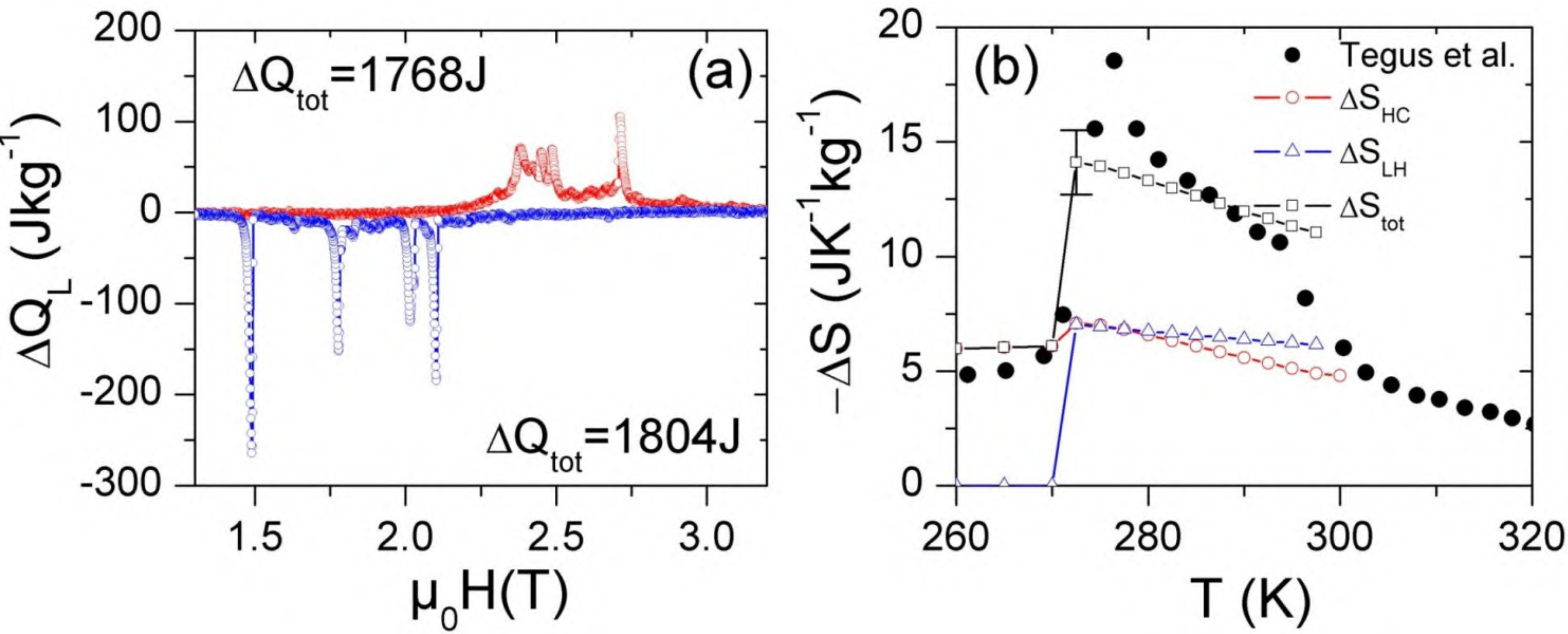

Microcalorimetry: ΔS_{LH}=1/2 ΔS_{total}

(Bulk methods estimate ΔS_{str} as somewhere between 40 and 60% of ΔS_{total} [2],[3])

[1] K. Morrison *et al.,* MRS Conference proceedings, **1310** 47-53 (2011).
[2] G.J. Liu *et al.*, *Appl. Phys. Lett.* **88**, 212505 (2006).
[3] V.K. Pecharsky *et al.*, *J. Magn. And Magn. Mater.* **321**, 3541-3547 (2009).

Approaching the Critical Point

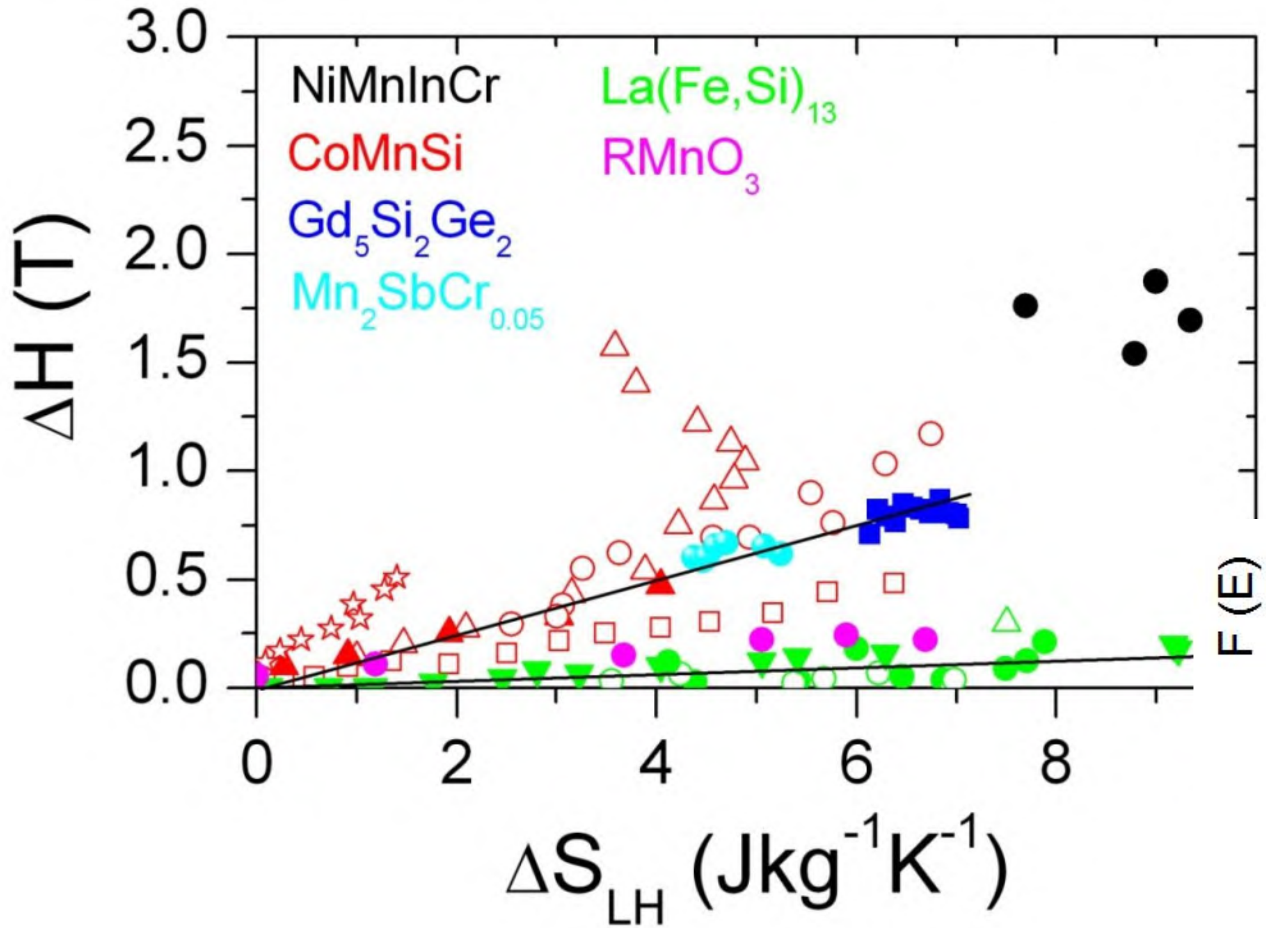

Aim:
Maximise ΔS
whilst limiting ΔH

Coupling to a structural phase transition significantly enhances the entropy change, but at what cost?

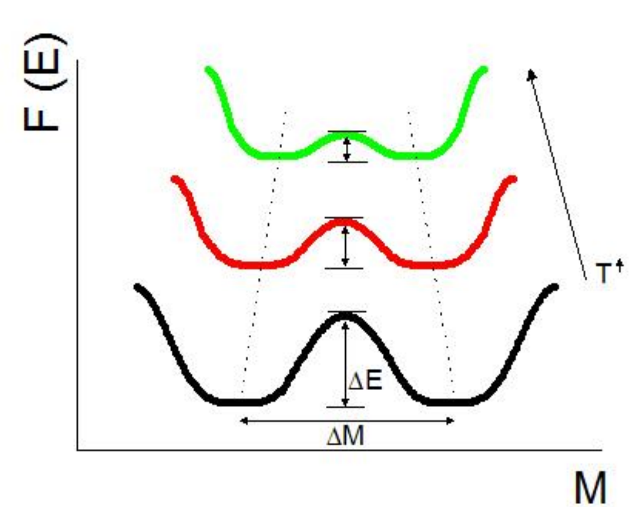

K. Morrison & L.F. Cohen, *Metallurgical and Materials Transactions E* **1** 153-159 (2014)

$LaFe_{13-x}Si_x$

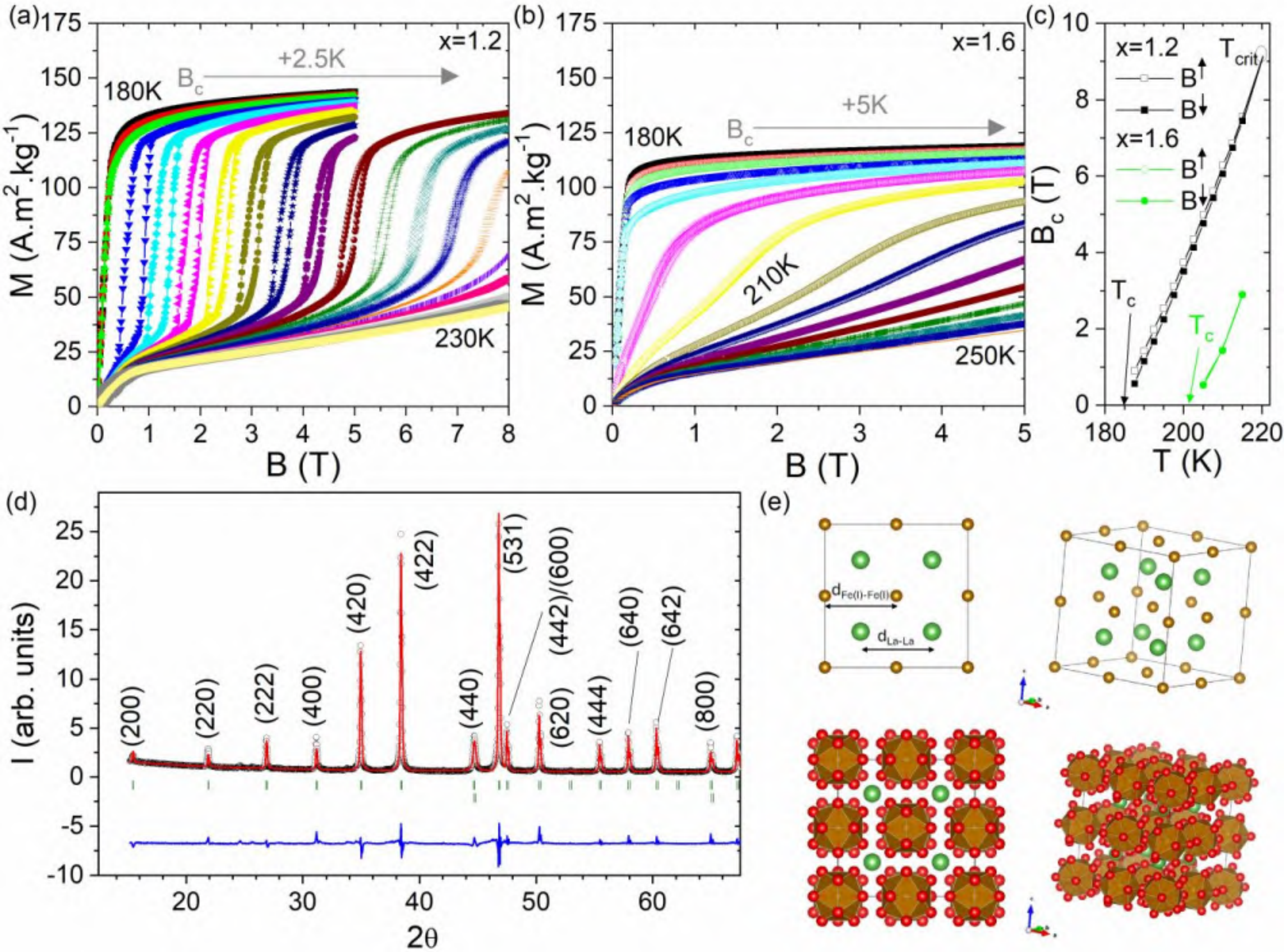

FOPT with tricritical point:

- x = 1.2 as a function of T, B

SOPT:

- x = 1.6 as a function of T

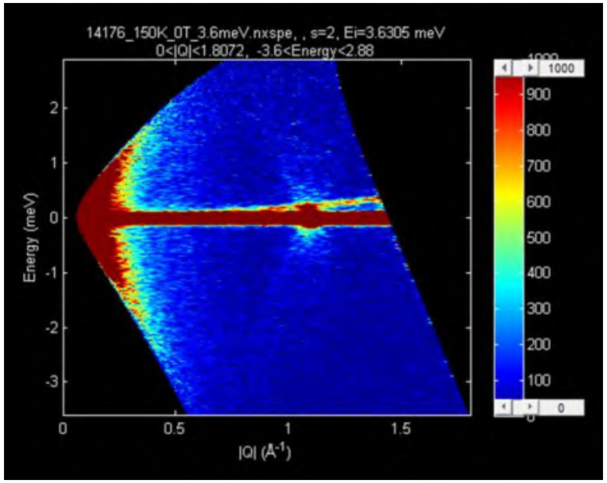

K. Morrison *et al., Adv. Physics Research* **3** 2400008 (2024)

Want to know more on materials?
See ESM 2013, Karl Sandeman.
Magneto-caloric materials

The tri-critical point

This type of behavior, where three critical lines come together at a point, is rather exceptional in nature (we shall mention some other examples below) and we therefore propose a special name: tricritical point.

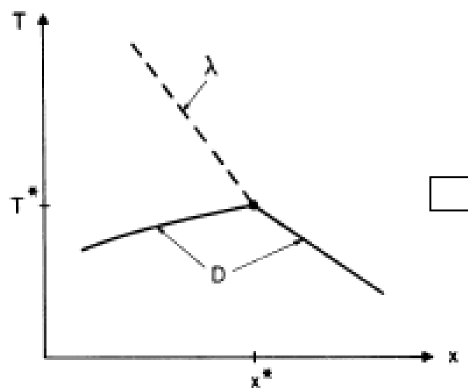

FIG. 1. Phase diagram (schematic) for He^3–He^4 mixtures near the critical mixing point. The two-fluid coexistence curve is labeled D and the dashed curve is the line of lambda transitions.

η, $\Delta = \mu_3 - \mu_4$

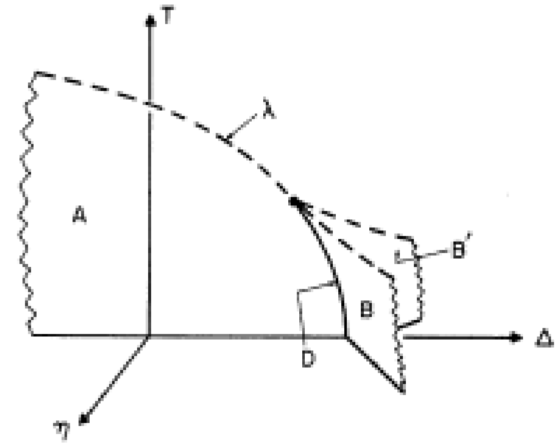

FIG. 2. Phase diagram (schematic) for He^3–He^4 mixtures in $T\Delta\eta$ space. Note that only the $T\Delta$ plane with $\eta = 0$ is experimentally accessible.

[1] R B Griffiths, *Phys. Rev. Lett.*, **24**, 715 (1970).

Universal Scaling

$$\Delta S_{Max} = \int_0^{H_2} \left(\frac{\partial M(T,H)}{\partial T} \right)_H dH$$

$$h = \Delta S_{Max} / \Delta S_{Max}^{Peak}$$

$$\theta = \begin{cases} -\dfrac{T - T_c}{T_{r1} - T_c} & T \leq T_c \\ \dfrac{T - T_c}{T_{r2} - T_c} & T > T_c \end{cases}$$

PHYSICAL REVIEW B 81, 224424 (2010)

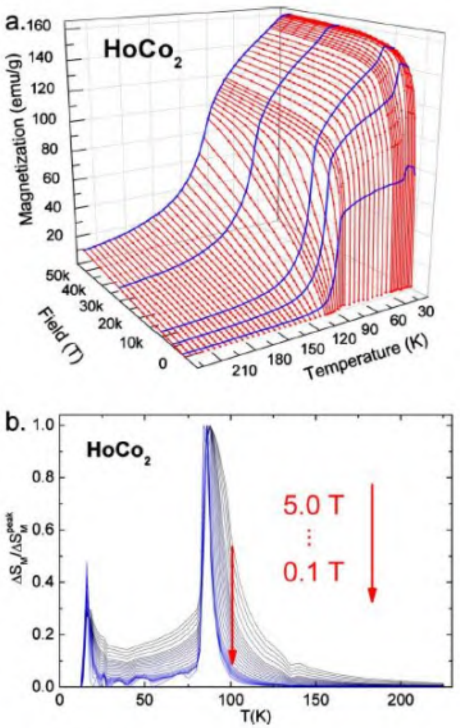

FIG. 1. (Color online) (a) Magnetization measurements as function of field for different temperatures for $HoCo_2$. The values of applied field during the measurement were 0, 0.1, 0.2, 0.3, 0.4, 0.5, 0.6, 0.7, 0.9, 1.0, 1.2, 1.4, 1.6, 1.8, 2.0, 2.2, 2.4, 2.6, 2.8, 3.0, 3.5, 4.0, 4.5, and 5.0 T. (b) Normalized entropy change versus temperature for different applied fields for $HoCo_2$.

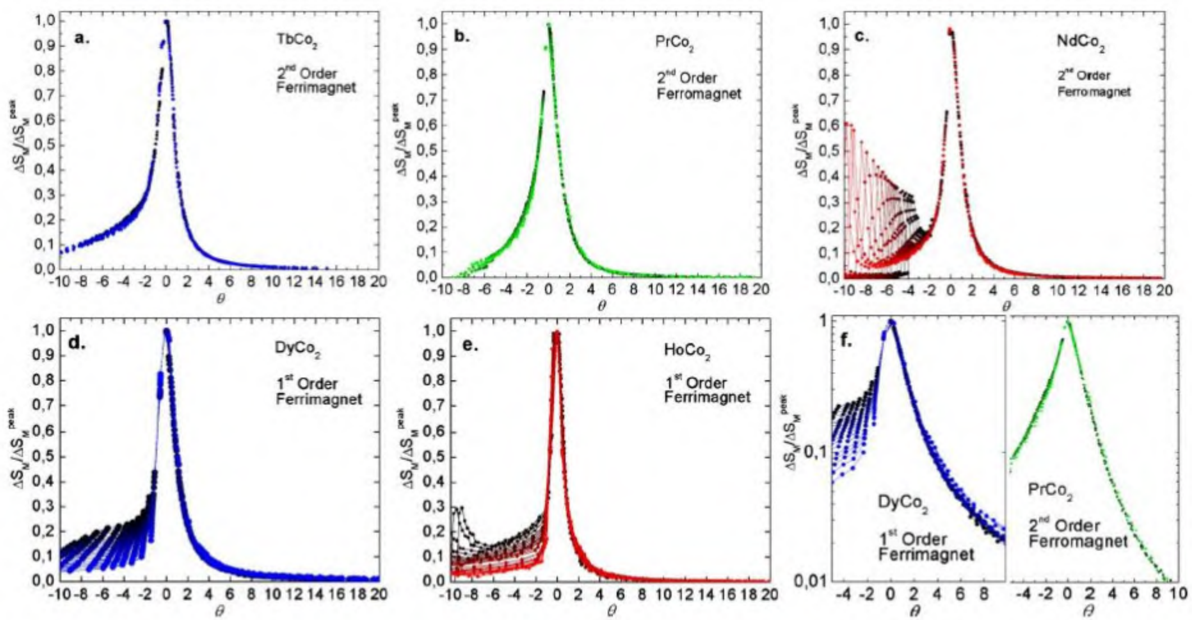

FIG. 2. (Color online) Normalized entropy change as a function of the rescaled temperature θ for the cobalt Laves phases studied in this work. A universal curve for the second-order phase transitions of $TbCo_2$ (panel a), $PrCo_2$ (panel b), and $NdCo_2$ (panel c) is demonstrated while a breakdown of the universal curve for the first order phase transitions of $DyCo_2$ (panel d) and $HoCo_2$ (panel e) can be observed. The panel f shows a comparison of the rescaled curves for $PrCo_2$ and $DyCo_2$ (vertical axis in logarithmic scale).

H.E. Stanley, *Rev. Mod. Phys.* **71**, S358 (1999)
C. Bonilla et al, PRB **81**, 224424 (2010)
V. Franco et al, J. Phys. Condens. Matter **20**, 285207 (2008)
V. Franco et al., Int. J. Refrig. 33, 465-473 (2010)

Universal Scaling

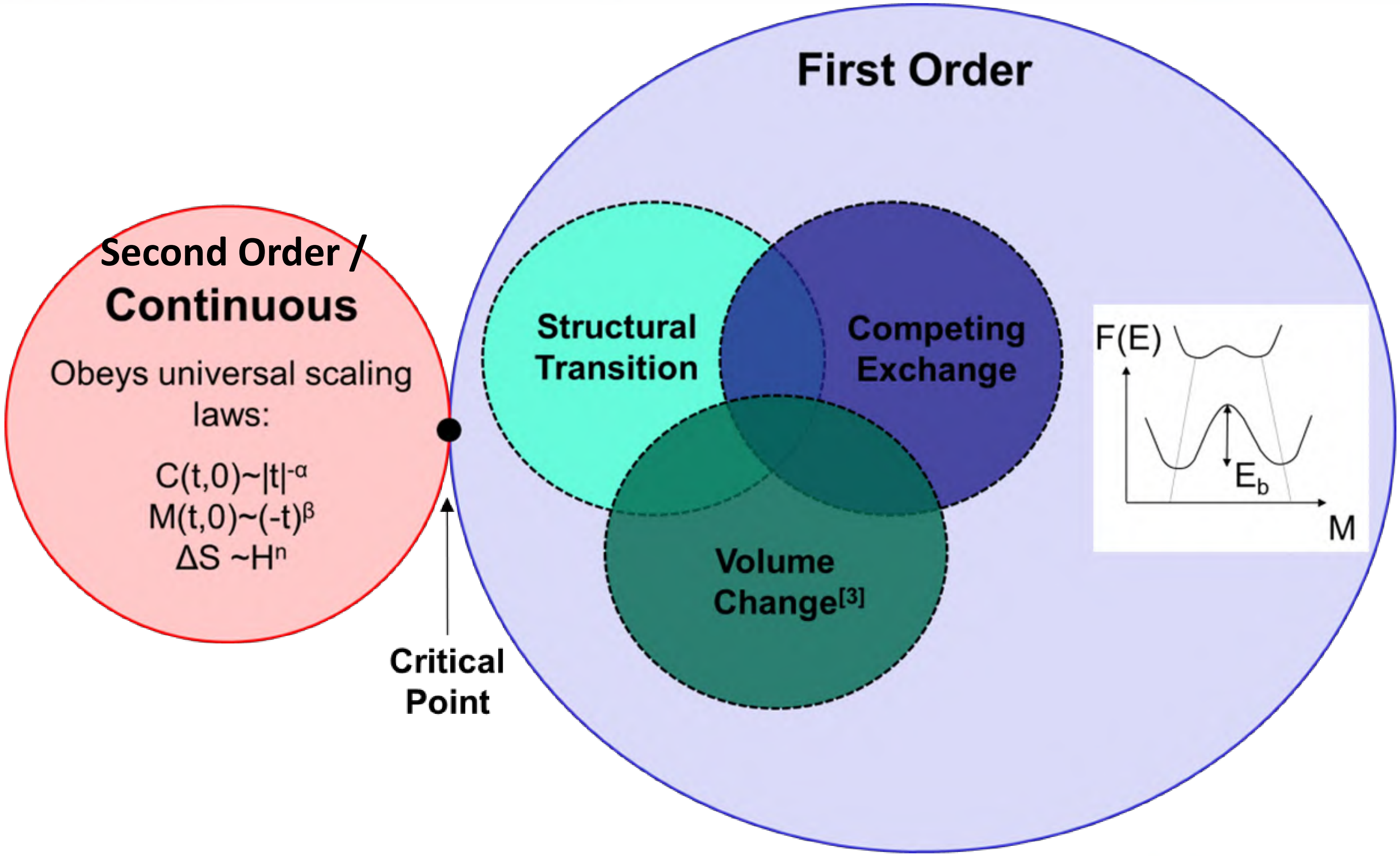

H. Oestereicher and F.T. Parker, *J. Appl. Phys.* **55** 4334 (1984)
V. Franco et al., *Appl. Phys. Lett.* **89**, 222512 (2006)

The Banerjee Criterion

Landau Free Energy Expansion

$$\frac{H}{M} = A + BM^2 + CM^4 + DM^6 + \cdots$$

Banerjee Criterion:
(Landau only)

$$B < 0$$

Shimizu Criterion:
(Landau+spin fluctuations)

$$\frac{3}{16} < \frac{AC}{B^2} < \frac{9}{20}$$

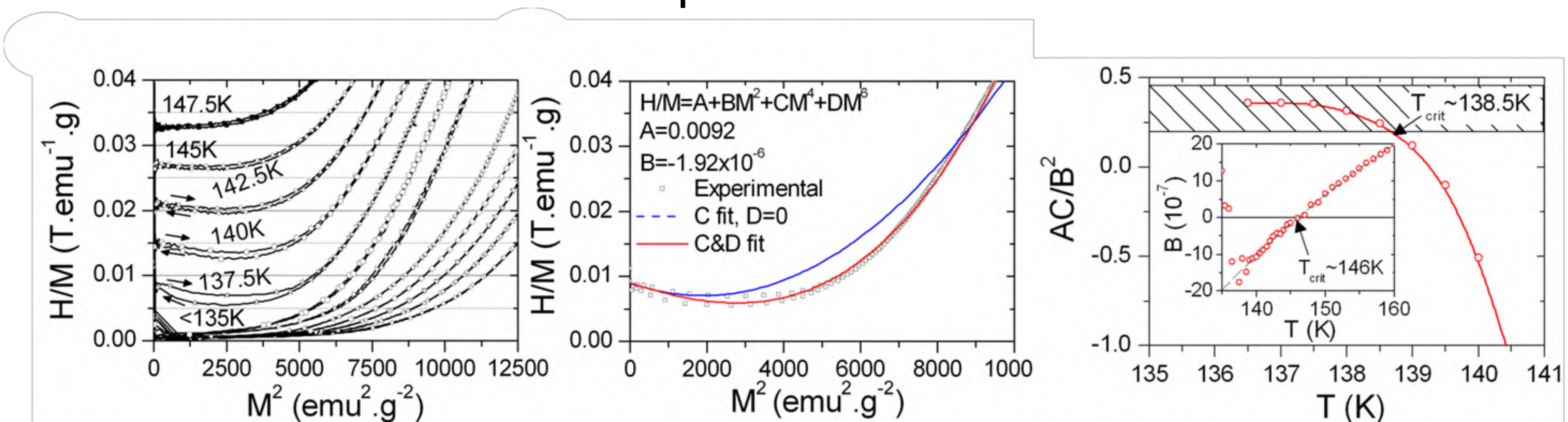

Figure 1 – Results of Landau fitting to isothermal magnetisation data. Left: Arrott plots of magnetisation data for 2.5 K increments from below T_c (~135.5 K) to 147.5 K. Centre: Example of Landau fitting at 137.5 K. Right: Temperature variation of the quantity AC/B² where A, B, and C are parameters extracted from Landau fitting. Inset shows B as a function of temperature. Note that the Shimizu criterion indicates T_{crit}=138.5 K whereas the Banerjee criterion indicates T_{crit}=146 K.

K. Morrison, *et al., Phys. Rev. B*, **87**, 134421 (2013)

Universal Scaling

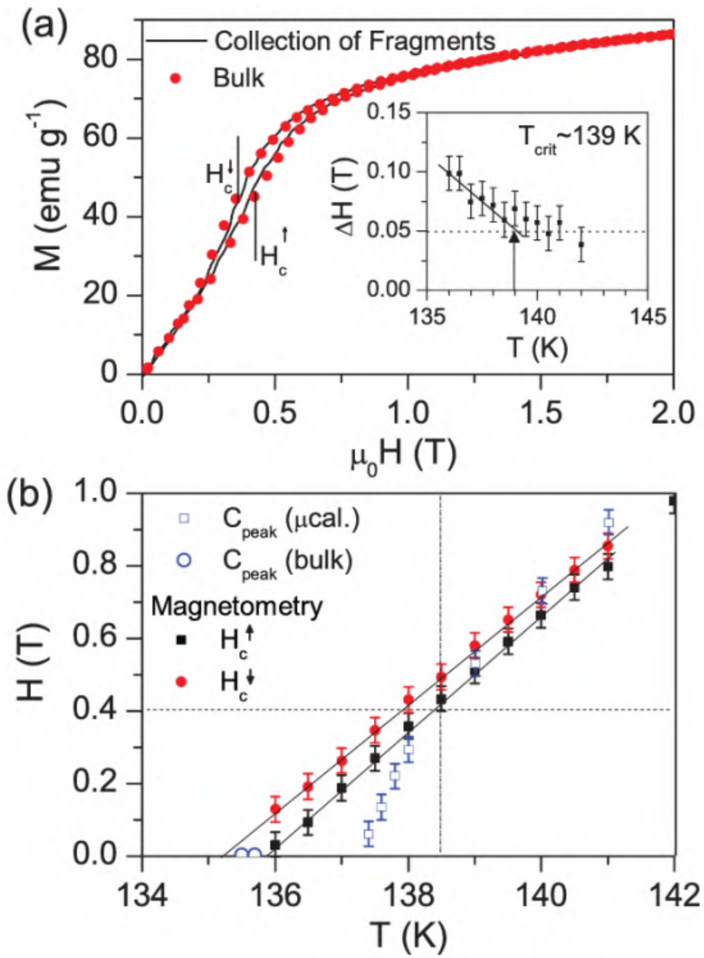

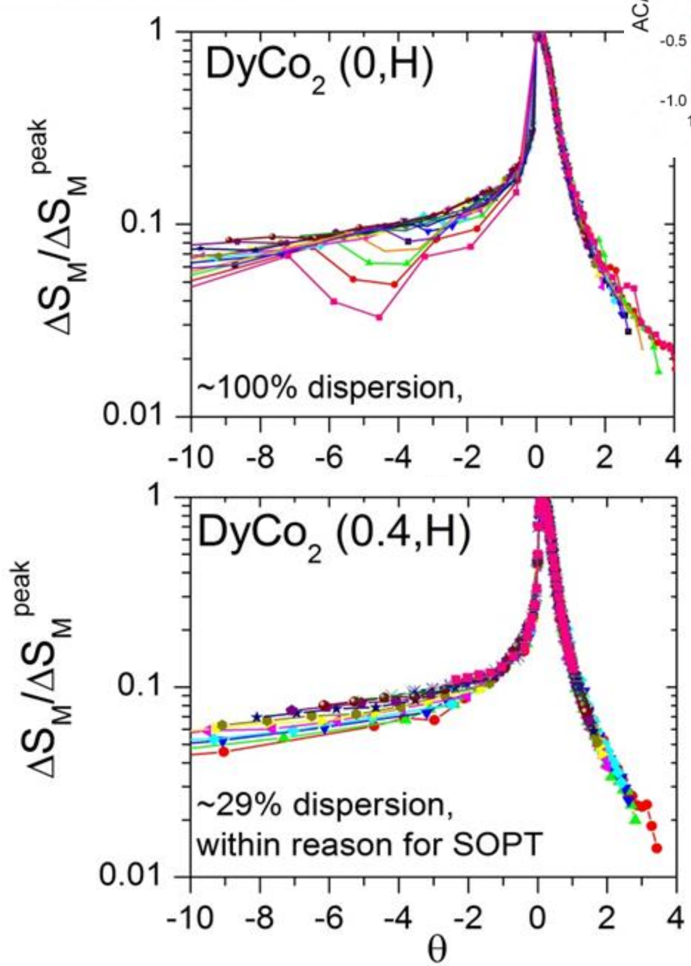

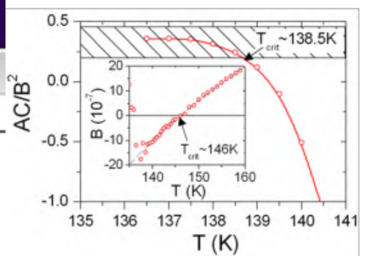

Thermal Engineering: Next Challenge?

- ΔS , ΔT_{ad}
- H_c, ΔH

Several potential material systems
e.g. $La(Fe,Si)_{13}$ $MnFe(P,Si)$

- Cost
- Manufacturability

Engineering problem unique to each system

- Tunability

Tailor T_c, κ^1 to optimise the working performance

Want to know more?: See ESM 2021, Oliver Gutfleisch
Magneto (and multi-)caloric materials for efficient refrigeration

J. Lyubina *et al.*, *Adv. En. Mater.*, **2**, 1323-1327 (2012)
J.A. Turcaud *et al.*, *Scripta Mater.*, **68**, 510-513 (2013)

Thermal Engineering

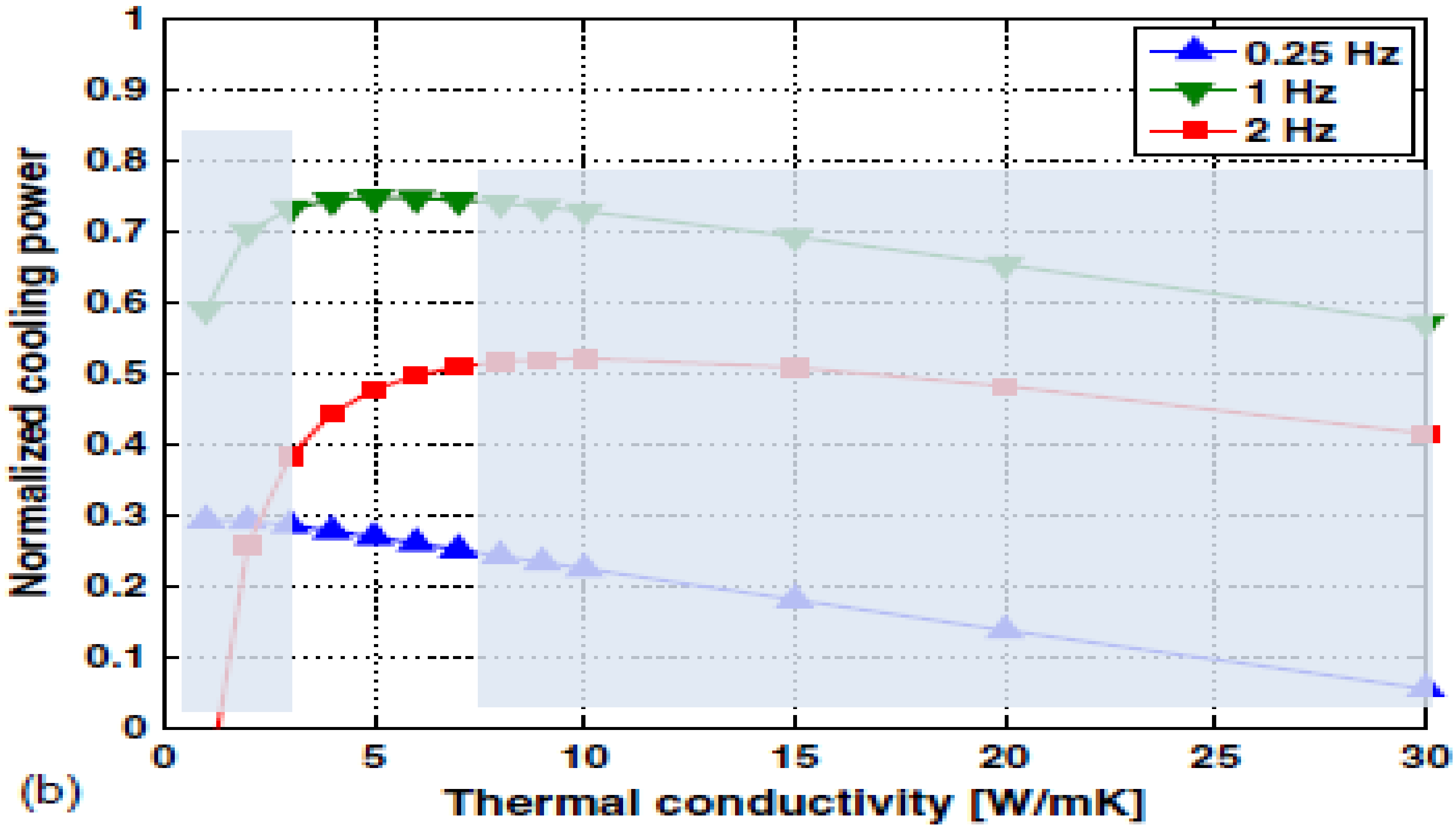

Nielsen & Engelbrecht, *Journal of Physics D: Applied Physics*, **45**, 145001 (2012)

Thermal Engineering

Optimise κ
Improve cycling stability

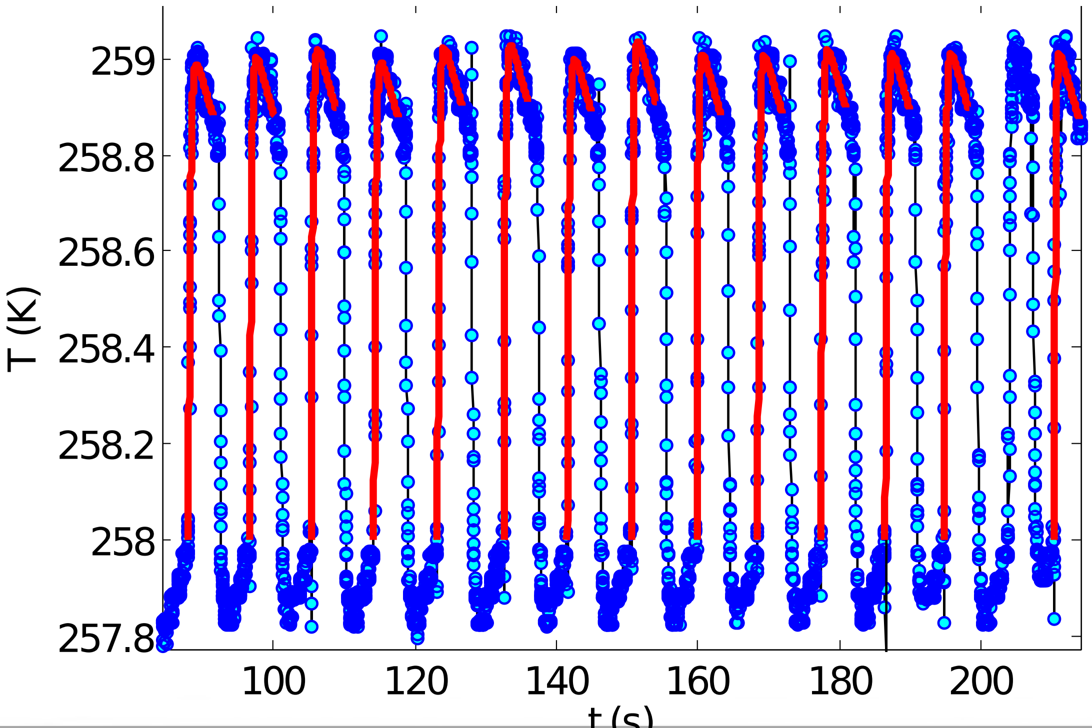

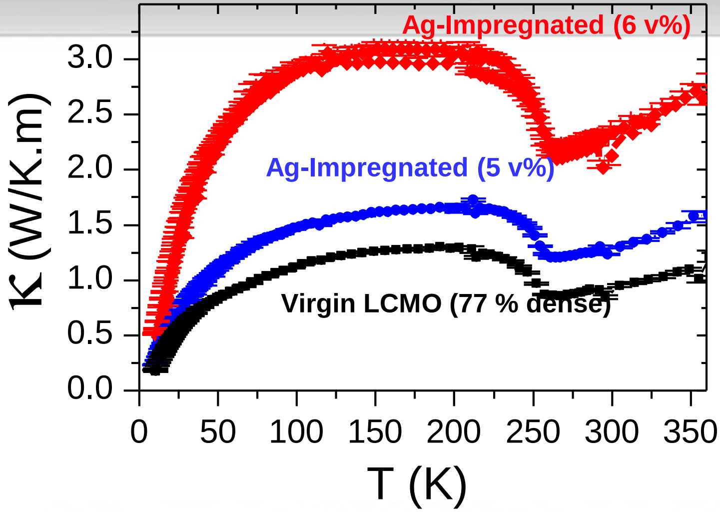

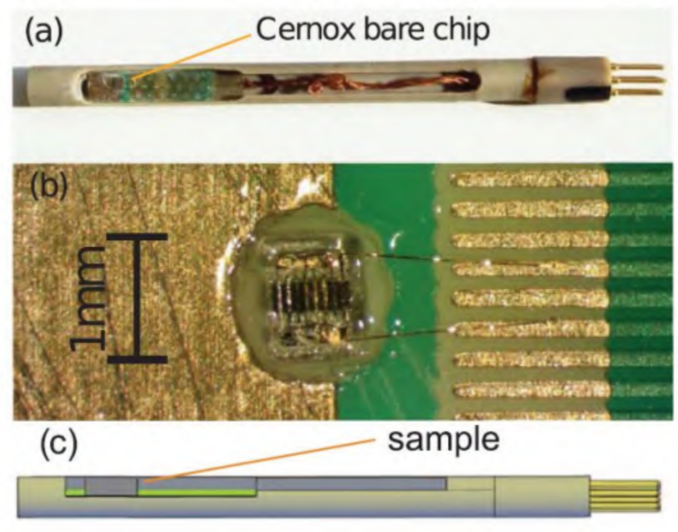

J. Lyubina *et al.*, *Adv. En. Mater.*, **2**, 1323-1327 (2012)
J.A. Turcaud *et al.*, *Scripta Mater.*, **68**, 510-513 (2013)
G. Porcari *et al.*, *Rev Sci Instrum.* **84**, 073907 (2013)

TCCbuilder:

an open-source tool for the analysis of thermal control elements and thermal control circuits

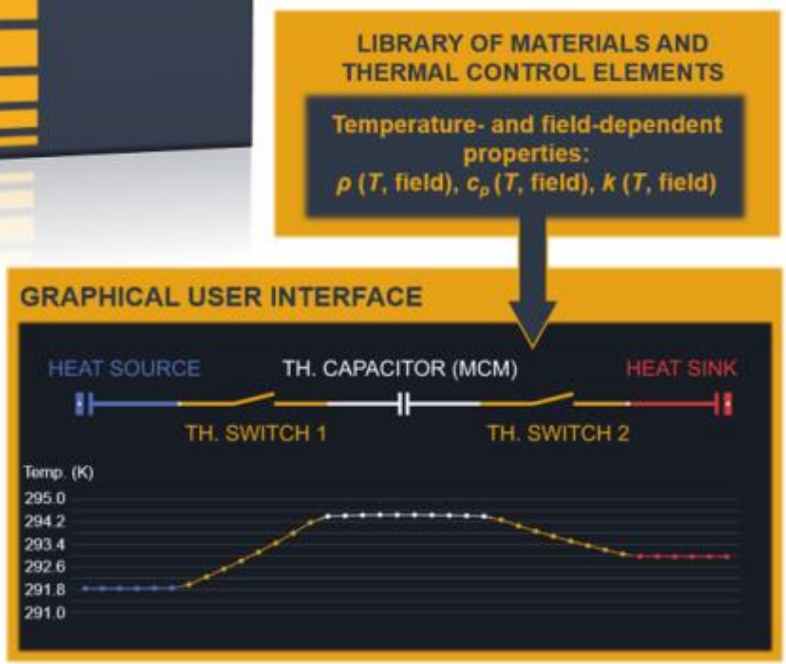

Online workshop

on TCCbuilder usage

Thursday, September 5th 2024
2pm CEST

(Registration is required, but free of charge)

Registration by 1st September

UNIVERSITY OF LJUBLJANA
Faculty of Mechanical Engineering

LAHDE
LABORATORY FOR REFRIGERATION AND DISTRICT ENERGY

Applications – Ubiblue (now Magnoric)

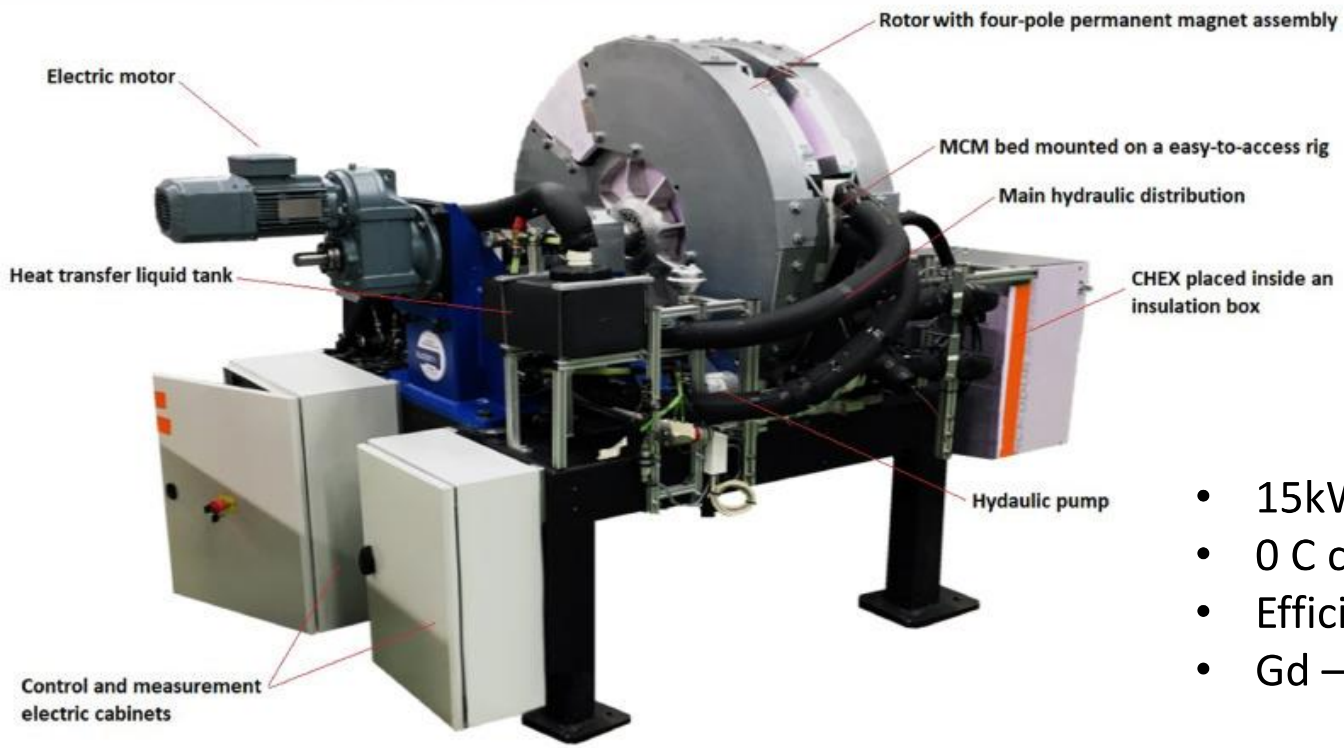

- 15kW
- 0 C cold temperature
- Efficiency 60% Carnot COP
- Gd – Gd-Er segments to tailor T_c

Int. J. Refrig. **122**, 256-265 (2021)

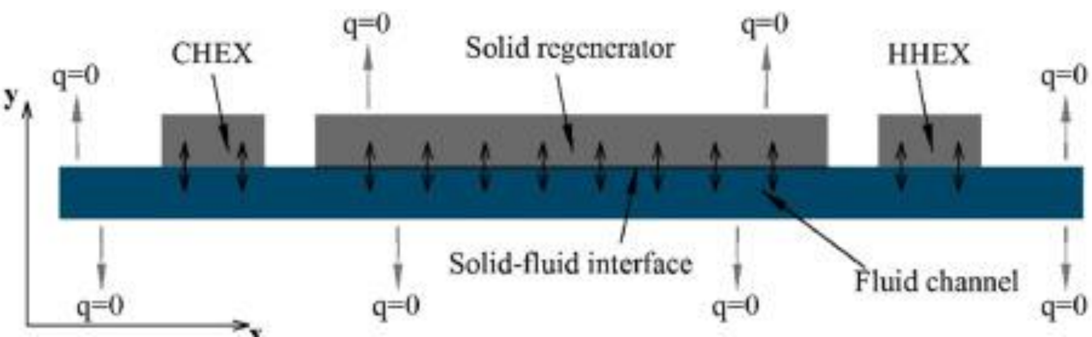

Applications - MagnoTherm

ESM 2021, Oliver Gutfleisch
Magneto (and multi-)caloric materials for efficient refrigeration

Polaris: 80 L beverage cooler

Double door: 1000L capacity commercial refrigerators

Manual (handcrank) fridge

Applications: Energy Harvesting

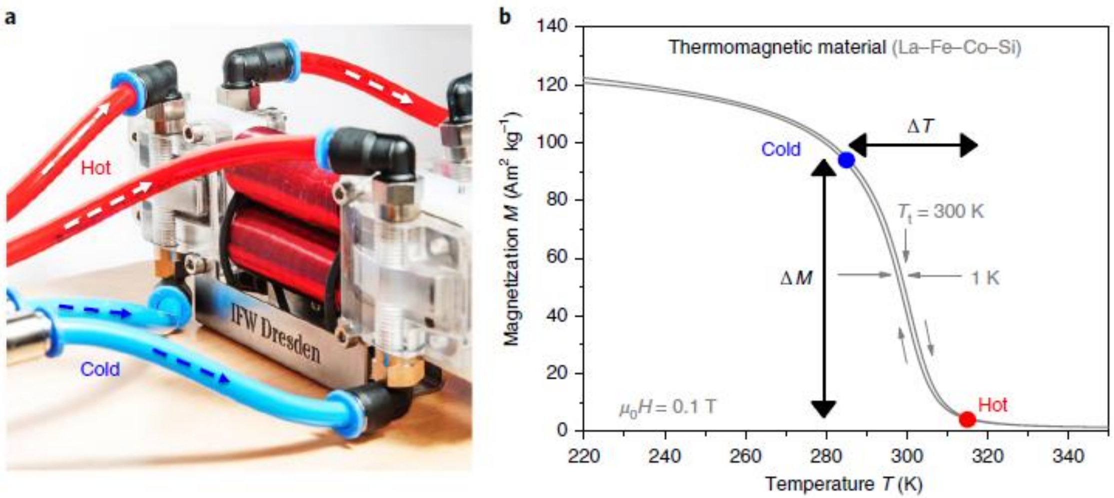

Low grade heat
Optimum frequency 1 Hz
Efficiency 1.7x10^{-3} % of η_{Carnot}

A. Kitanovski, *Advanced Energy Materials* **10**, 1903741 (2020)

A. Waske *et al.*,
Nature Energy **4**, 68-74 (2019)

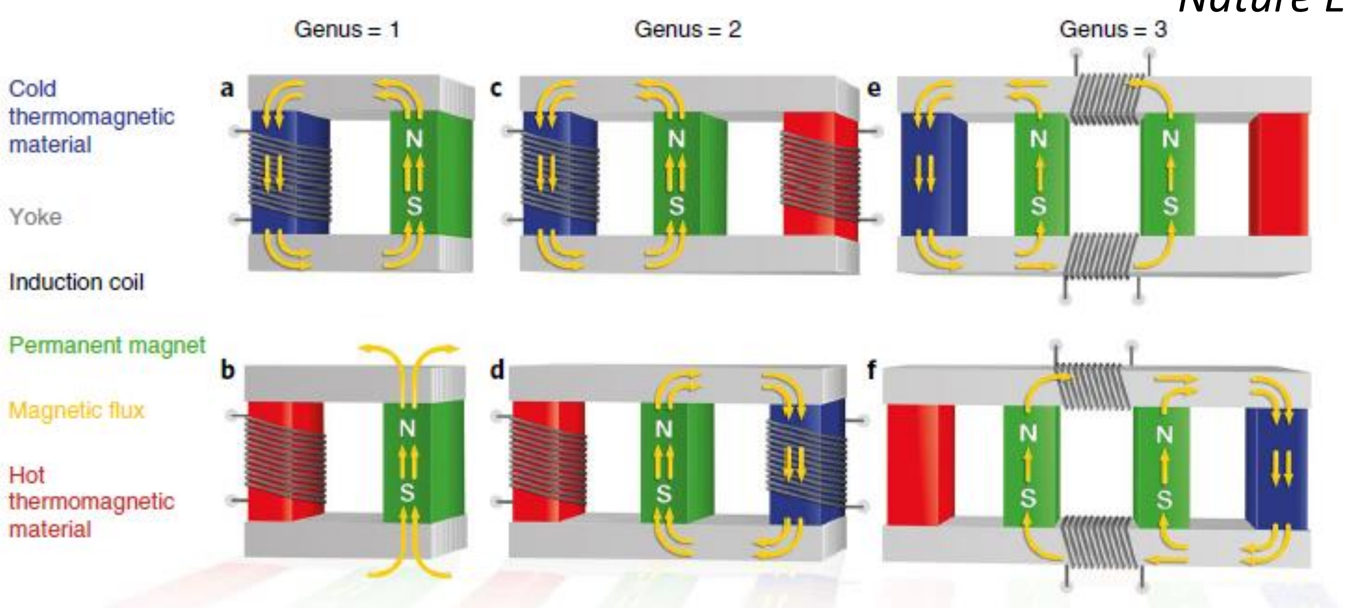

HEAT4ENERGY EU project launched in 2024

Applications: Energy Harvesting

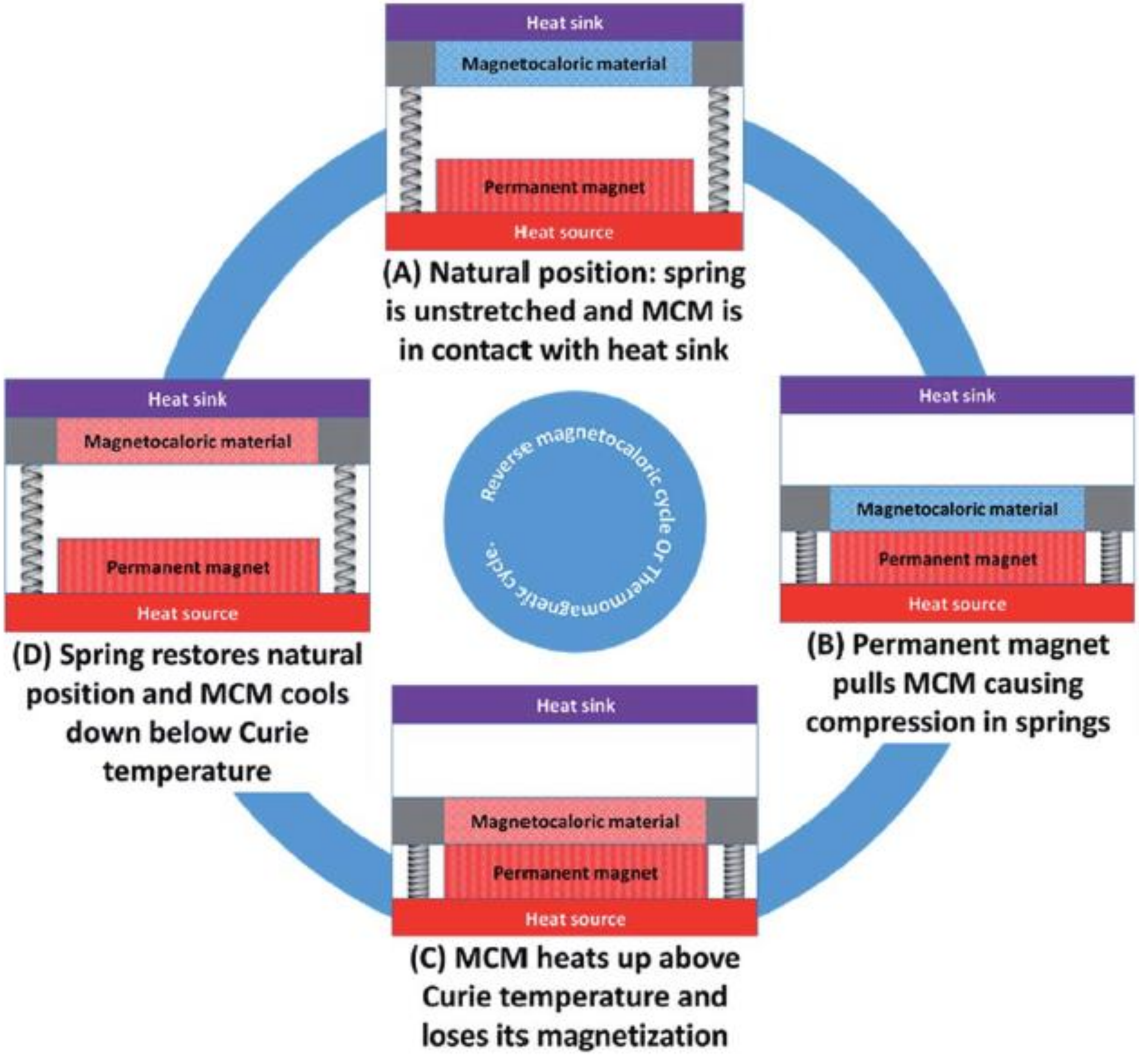

M. Ujihara, G.P. Carman, and D.G. Lee, *APL* **91**, 093508 (2007)

- 1.85-3.61 mW/cm^2 for ΔT=50K.
- Predicted as high as 36.1 mW/cm^2 if thermal contacts improved

R. A. Kishore and S. Priya, *Sustainable Energy and Fuels*, **1**, 1899 (2017)

Magnetocaloric Effect (Magnetic Refrigeration / Energy Harvesting)

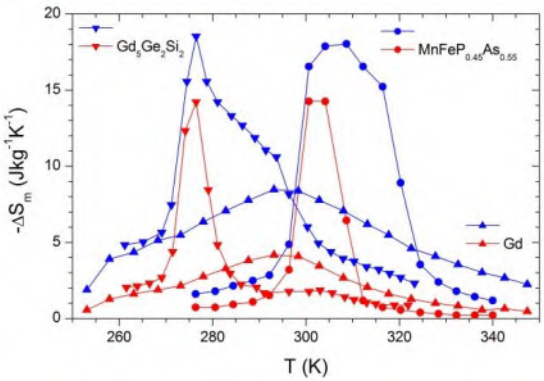

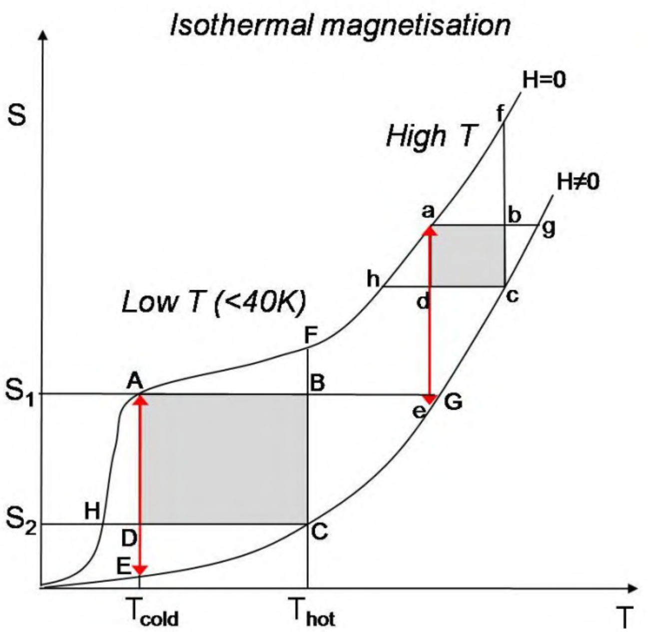

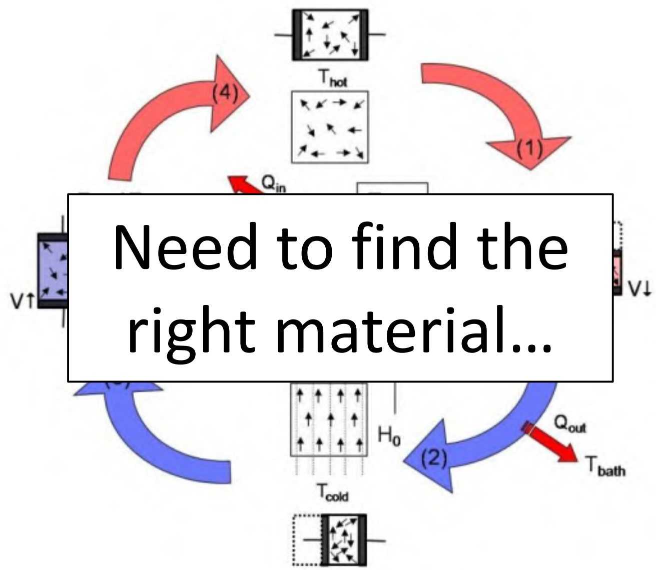

Need to find the right material…

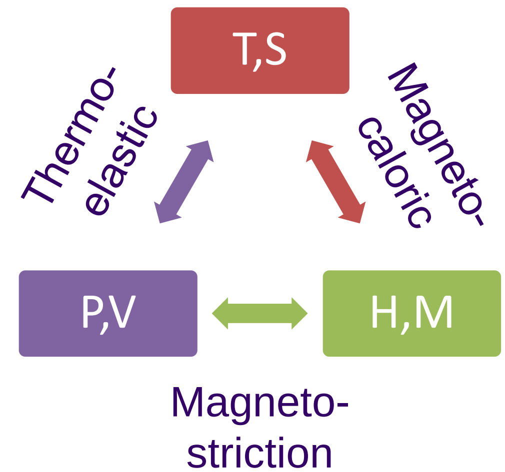

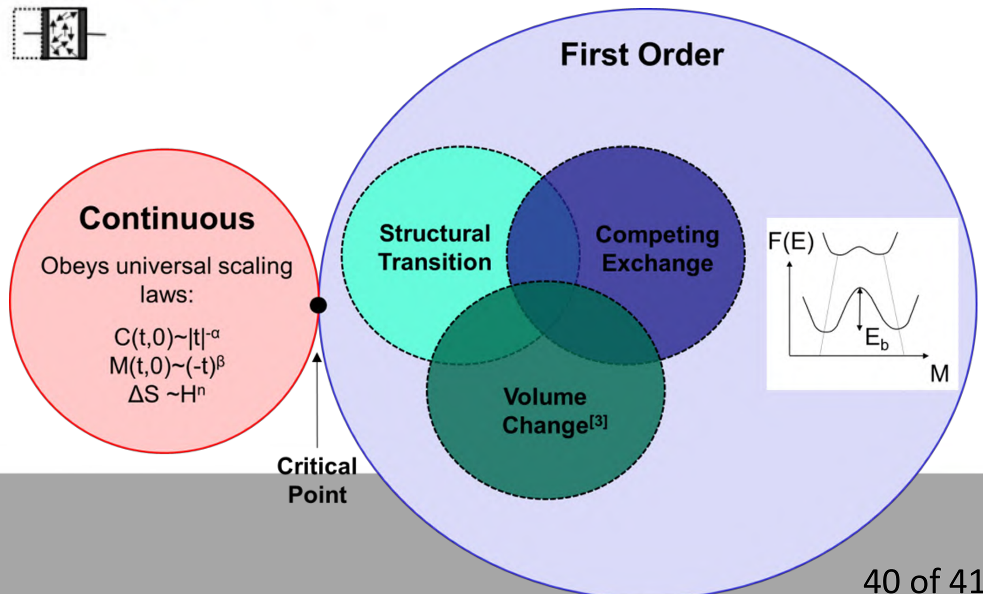

Any Questions?

Imperial College
A. Berenov, J. Turcaud,
M. Bratko, K.G. Sandeman,
Z. Gercsi, J. Lyubina,
E. Lovell, D.A. Caplin,
L.F. Cohen

Ames Laboratory
V.K. Pecharsky,
K.A. Gschneidner,
Y. Mudryk

EPSRC Engineering and Physical Sciences Research Council

www.sseec.eu
SSEEC
Solid State Energy Efficient Cooling

Vacuumschmelze
A. Barcza

IFW Dresden
J.D. Moore

TU Darmstadt
O. Gutfleisch, K. P. Skokov

University of Parma
G. Porcari

Loughborough University
J. Betuoras, A. Caruana